Secondary bile acid production by gut bacteria promotes Western diet-associated colorectal cancer

Esther Wortmann[*1], Annika Osswald[*2], David Wylensek[1], Wei Liang[3], Nicole Treichel[1], Fabian Schumacher[4], Colin Volet[5], Silke Matysik[6], Karin Kleigrewe[7], Michael Gigl[7], Sascha Rohn[8], Burkhard Kleuser[4], Gerhard Liebisch[6], Rizlan Bernier-Latmani[5], Angelika Schnieke[3], Krzysztof Flisikowski[3], Soeren Ocvirk[**,2,9], Thomas Clavel[**, ***,1]

[1]Functional Microbiome Research Group, Institute of Medical Microbiology, RWTH University Hospital, Aachen, Germany.

[2]Intestinal Microbiology Research Group, German Institute of Human Nutrition, Potsdam-Rehbruecke, Nuthetal, Germany.

[3]Chair of Livestock Biotechnology, Weihenstephan School of Life Science, Technical University of Munich, Freising, Germany.

[4]Institute of Pharmacy, Department of Pharmacology and Toxicology, Freie Universität Berlin, Berlin, Germany.

[5]Environmental Microbiology Laboratory, School of Architecture, Civil and Environmental Engineering, École Polytechnique Fédérale de Lausanne, Lausanne, Switzerland.

[6]Institute of Clinical Chemistry and Laboratory Medicine, University Hospital of Regensburg, Regensburg, Germany.

[7]Bavarian Center for Biomolecular Mass Spectrometry, School of Life Sciences, Technical University of Munich, Freising, Germany.

[8]Institute of Food Technology and Food Chemistry, Technische Universität Berlin, Berlin, Germany.

[9]ZIEL – Institute for Food and Health, Technical University of Munich, Freising, Germany.

*: shared first authors, **: shared last authors, ***: corresponding author

Conflict of Interest

The authors declare no potential conflicts of interest.

Abstract

Intake of Western diet stimulates bile acid (BA) production and their conversion to secondary BAs by 7α-dehydroxylating (7αDH+) bacteria in the colon. Increased levels of 7αDH+ bacteria and the secondary BA deoxycholic acid (DCA) have been associated with sporadic colorectal cancer (CRC). However, causal proof of their tumour-promoting effects under detrimental dietary conditions is lacking. Therefore, we performed feeding studies in a transgenic pig model of CRC combined with multi-omics analyses and gnotobiotic mouse studies. Western diet worsened the disease phenotype in *APC*$^{1311/+}$ pigs. This was accompanied by increased levels of DCA and colonic epithelial cell proliferation, which was counteracted by using the bile acid-scavenging drug colestyramine. Using a gnotobiotic mouse model of CRC, we demonstrate that colonisation with different 7αDH+ bacterial isolates increased colonic tumour loads. These complementary approaches present clear evidence for the causal role of microbiome-derived DCA production in CRC, opening avenues for future preventive strategies.

Introduction

Colorectal cancer (CRC) has one of the highest incidences and mortalities among all cancer types worldwide, with approximately 1.9 million new cases and 0.9 million deaths in 2020 [1]. Besides genetic factors, including mutations in the tumour-suppressing adenomatous polyposis coli (*APC*) gene, sporadic CRC risk is predominantly influenced by environmental and lifestyle factors, including diet and the gut microbiome [2–4]. There is convincing evidence for a positive association between CRC risk and Western-style diets rich in fat and red/processed meat, whilst high-fibre intake is negatively associated with CRC risk [5–7]. In healthy individuals in South Africa, who have a very low CRC risk, a 2-weeks diet switch from a traditional high-fibre/low-fat to a Western-style low-fibre/high-fat dietary pattern altered gut microbiota composition and metabolism, leading to an increase in markers associated with CRC risk such as intestinal epithelial cell proliferation and infiltration of CD3+ and CD68+ immune cells [8]. Alaskan Native people, who traditionally consume a diet rich in fat and have the world's highest risk for CRC, have a gut microbiota characterised by lower diversity and metabolic adaption to bile acid (BA) metabolism [9].

High fat intake stimulates BA synthesis by the host, resulting in increased amounts of BAs entering the colon, where they are converted to secondary BAs by gut bacteria. Elevated levels of secondary BAs, in particular deoxycholic acid (DCA), were detected in faeces of CRC patients and healthy cohorts at high CRC risk, and they correlated with higher occurrence of BA-inducible (*bai*) genes involved in BA dehydroxylation (DH) by gut bacteria [10–14]. In the murine *Apc*$^{min/+}$ model, a diet supplemented with the primary BA cholic acid (CA, 0.4% w/w, 12 weeks), the precursor of DCA, increased the number and size of intestinal tumours [15]. This effect was prevented by antibiotic treatment, suggesting a contribution of the gut microbiota to CA-associated tumorigenesis in this CRC model. Oral intake of DCA promoted tumour development in the proximal colon of wild type mice (0.2% w/w in diet for up to 10 months) [16], high-grade dysplasia in AKR/J mice treated with azoxymethane (AOM) (0.25% w/w in diet for >10 weeks) [17] and higher numbers of intestinal tumours in *Apc*$^{min/+}$ mice (0.2% w/v in drinking water for 12 weeks) [18]. Faecal microbiota transplantation from DCA-treated *Apc*$^{min/+}$ donor mice to microbiota-depleted *Apc*$^{min/+}$ recipients on a control diet induced increased intestinal tumour numbers [19]. However, in these studies, mice were fed with DCA directly, which does not mirror physiological conditions, or DCA levels were not analysed. Moreover, the *Apc*$^{min/+}$ mouse model develops tumours primarily in the small intestine, which does not reflect the location of tumorigenesis in humans and contrasts to colon being the main site of secondary BAs production [20,21]. Hence, clear evidence for a causal role of microbially produced DCA in relation to diet and underlying mechanisms in colonic tumorigenesis is still lacking.

Here we investigated the role of secondary BA production by gut bacteria in CRC based on a multi-layer approach using dietary interventions in transgenic pigs, gnotobiotic mouse models of CRC, and a combination of multi-omics and cultivation methods. This allowed us to span analyses from microbial community level to detailed investigations of specific microbiota members involved in the conversion of BAs, collectively demonstrating a diet-driven, tumour-promoting function of secondary BA-producing bacteria.

Results

Western diet aggravates polyp state in the *APC*$^{1311/+}$ pig model

Pigs and humans are omnivores and share similarities in their intestinal microbiota, gastrointestinal anatomy, physiology, and metabolic processes. This has made the pig an ideal model to study gastrointestinal diseases [22,23]. In contrast to transgenic mouse models based on the *Apc* gene, *APC*$^{1311/+}$ pigs recapitulate key features of human disease, including the location of tumours in the large intestine [24], disease progression, and differences in severity within families [25].

Hence, to investigate the role of a Western diet on the development of CRC under controlled conditions in a preclinical setting, we performed a feeding intervention in *APC*$^{1311/+}$ pigs. The animals were fed (1 kg/d) either a control diet (CTRL) or an experimental diet enriched in red meat and lard (RL diet) for 3 months (see experimental design in **Fig. S1a** and diet composition in **Table S1**). Whilst control *APC*$^{1311/+}$ pigs showed a stable disease phenotype, both the number and size of colonic polyps were significantly increased in the RL diet group (**Fig. 1a**). Higher levels of Ki67+ cells in distal colonic crypts indicated increased proliferation of the epithelium (**Fig. 1b**).

Western diet alters microbiota profiles and promotes high levels of secondary bile acids in *APC*$^{1311/+}$ pigs

To assess the effects of the experimental feeding on the gut microbial ecosystem, faecal samples were analysed by 16S rRNA gene amplicon sequencing before and after intervention. *Alpha*-diversity analysis revealed a trend towards increased richness and Shannon effective counts in the CTRL group, which was not observed in the RL group, including a sharp drop in diversity in the two pigs with most severe disease progression (**Fig. 2a**). According to *beta*-diversity analysis, the microbiota structure between CTRL and RL pigs overlapped at the beginning of the feeding trial (4 months) but diverged after experimental feeding (7 months, **Fig. 2b**). At the level of dominant bacterial families, a decrease in *Prevotellaceae* and *Acidaminococcaceae* over time was observed in both groups, but it was significantly more pronounced in RL pigs (**Fig. 2c**). Whilst *Fibrobacteraceae* increased in the CTRL group, RL pigs were characterised by a significant increase in *Desulfovibrionaceae*.

Besides diet-induced effects on microbiota diversity and composition, changes in faecal metabolites were assessed. Targeted LC-MS/MS measurements showed that primary BAs were overall increased in RL pigs after dietary intervention, primarily due to glycocholic acid (GCA), which was not detected in the CTRL group (**Fig. 2d**). Total concentrations of secondary BAs were slightly higher in the CTRL group, mainly driven by hyodeoxycholic acid (HDCA), shown by others to suppress epithelial proliferation [26]. In contrast, levels of the CRC-associated secondary BAs DCA and 12-keto-litocholic acid (12-KLCA) were substantially higher in the RL group (**Fig. 2e**).

The bile acid sequestrant colestyramine limits Western diet-associated epithelial cell proliferation in the colon of *APC*$^{1311/+}$ pigs

Next, we investigated whether the increase in BAs contributed to the RL diet-induced phenotype in *APC*$^{1311/+}$ pigs. Therefore, a second feeding trial was carried out, including a third group fed the RL diet supplemented with the drug colestyramine (COL; 12g/d), a bile acid scavenger that makes BAs unavailable for bacterial transformation and enterohepatic circulation [27] (see experimental design in **Fig. S1b**). Whilst the number of polyps tended to decrease after intervention in all COL pigs (**Fig. 3a;** $p = 0.062$), their size varied markedly between individuals in this group (**Fig. 3b**). Moreover, the number and size of polyps in the CTRL and RL groups showed no consistent changes over time. However, immunohistochemistry staining of Ki67+ cells confirmed the proliferative effect of the RL diet in crypts of the distal colon, which was prevented by COL (**Fig. 3c** and **d**).

Targeted analysis of faecal BAs at the end of the feeding period showed higher total levels of primary and secondary BAs in RL and COL pigs (p.adj. = 0.068 and 0.066, respectively; Kruskal-Wallis), including higher concentrations of GCA (p.adj. = 0.05), allocholic acid (AlloCA) (p.adj. = 0.07), CA, and ursocholic acid (UCA) (p.adj. = 0.05) (**Fig. 4a**). Faecal concentrations of the secondary BAs DCA and 12-KLCA increased with RL diet feeding, whilst they tended to be less in the case of colestyramine treatment (**Fig. 4b**). Targeted measurements of BAs were complemented by a lipidomics approach. Levels of plant sterols were elevated in faecal samples from CTRL pigs and colestyramine tended to compensate for this effect in the case of cholestanol and 5-α sitostanol (**Fig. 4c**). In contrast, the levels of cholesterol and derivatives (**Fig. 4c**) as well as total fatty acids were highest in stool of COL pigs. The fatty acid (FA) difference was mainly driven by total

saturated and branched chain (iso and ante-iso) FA, whereas unsaturated FA and long chain FA (22-24) showed no significant differences (**Fig. 4d**).

Taken together, results from the two feeding trials in transgenic pigs provide interventional evidence for the positive association between Western dietary habits, elevated levels of secondary BAs, and polyp formation. Western diet-driven epithelial cell proliferation in the colon was prevented by treatment with the drug colestyramine. Colestyramine stimulated faecal excretion of lipids, which were most likely not available for the host and, in the case of BAs, for bacterial conversion into secondary BAs. To further demonstrate the causal implication of secondary BAs in CRC development, we then used gnotobiotic mouse models.

Microbially produced deoxycholic acid promotes epithelial cell proliferation and tumorigenesis in the colon

Germfree wildtype mice on a high-fat diet were colonised with a newly established simplified consortium of human gut bacteria, the BA-converting synthetic microbiota (BACOMI, **Fig. S1d**). BACOMI includes 7α-dehydroxylation activity (7αDH+) by *C. scindens* to produce DCA and can be compared to the condition without DCA when *C. scindens* is excluded from the consortium (7αDH-). Targeted qPCR analysis revealed a high relative abundance of 23.0 ± 2.9% (mean ± SD) for *C. scindens* in BACOMI-colonised mice and a relatively uniform colonisation pattern of the other bacteria after 3 months (**Fig. 5a**). Consistently, the presence of *C. scindens* caused high levels of secondary BAs, in particular DCA, which was not detected when 7αDH activity was lacking in the microbial consortium (**Fig. 5b**). DCA concentrations were higher in female than male mice when colonised by *C. scindens*. Interestingly, 7αDH activity and DCA enhanced the expression of genes within BA-dependent signalling pathways (**Fig. 5c**) and other genes known to be involved in tumorigenesis in the colonic epithelium (**Fig. 5d**). Furthermore, 7αDH activity was linked to higher numbers of Ki67+ epithelial cells in the colon (**Fig. 5e**).

To analyse whether 7αDH-mediated BAs affect colonic tumorigenesis, germfree wildtype mice on high-fat diet were colonised with BACOMI (including *C. scindens*) and then treated with AOM and dextran sodium sulphate (DSS). To consolidate these findings

independent of the 7αDH+ bacterial species, we performed additional experiments in mice colonised by *Extibacter muris* [28,29] instead of *C. scindens* (**Fig. 6c**). Following AOM/DSS treatment, *C. scindens* was present at higher relative abundance (50.3 ± 7.1%) when compared with untreated wildtype mice (**Fig. 5a**), suggesting favourable growth conditions for *C. scindens* under chemically induced colonic tumorigenesis (**Fig. 6b**). DCA was only detected in mice colonised with *C. scindens*, including higher levels in female mice (**Fig. 6d**). Levels of oxo-DCA were also higher in the caecal content of female mice when *C. scindens* was present. Despite these sex differences in secondary BA concentrations, bacterial 7αDH activity led to higher tumour numbers in the colon of nearly all mice (**Fig. 6f**). Stratification according to tumour size revealed significance for small tumours, which suggests early-stage promotion of tumorigenesis rather than tumour progression (**Fig. 6f**).

Compared with *C. scindens*-colonised mice*, E. muris* was less abundant, which was linked to a more uniform distribution of the remaining bacterial species (**Fig. 6c**). DCA was detected in caecum when 7αDH activity by *E. muris* was present and sex-specific differences (higher levels in females) were confirmed (**Fig. 6e**). Several other secondary BAs were significantly elevated when *E. muris* 7αDH was present (e.g., 12-oxo CDCA, HCA, TDCA or LCA). Interestingly, levels of the primary BA CA were higher in 7αDH- mice, indicating enhanced conversion in 7αDH+ mice. Similar to the effects of *C. scindens*, 7αDH activity by *E. muris* caused higher numbers of tumours in the colon, which was again linked primarily to small tumours (**Fig. 6g**).

Discussion

This study demonstrates the role of secondary BAs produced via gut bacterial 7αDH as tumour-promoting metabolites in experimental CRC. In contrast to non-physiological DCA supplementation in previous studies, we provide causal evidence linking the CRC risk-promoting effects of Western diets to functional adaptation of the gut microbiota. The experiments in *APC*$^{1311/+}$ pigs substantiate the clinical relevance of Western diet-mediated stimulation of microbial BA metabolism and suggest that promoting the excretion of BAs is a therapeutic option to limit their tumorigenic effects in the large intestine.

Bacterial 7αDH activity enhanced colitis-associated CRC in the gnotobiotic mice. This is an important experimental proof of previous observational data on higher numbers of 7αDH+ bacteria in faeces of CRC patients or individuals at high CRC risk [9–14]. It also provides physiologically relevant evidence for the tumour-promoting effects of secondary BAs in murine CRC models compared with previously tested oral DCA supplementation and observed effects in the small intestine [16–19]. Of note, 7αDH caused significantly higher numbers of small but not large colonic tumours in our gnotobiotic mouse experiments. This may indicate that DCA promotes cellular processes underlying tumour initiation rather than progression in the colonic epithelium of susceptible hosts.

There are multiple possible mechanisms for the tumour-promoting effect of DCA. For instance, it was shown to stimulate cancer stemness in colonic epithelial cells by modulating β-catenin signalling [30,31]. It also triggered proliferation and DNA damage in *Apc*$^{Min/+}$ Lgr5+ intestinal stem cells by antagonizing the BA receptor Fxr [32]. Moreover, oral administration of DCA and high-fat diet-associated secondary BAs promoted proliferation of Lgr5+ stem cells via the BA receptor Tgr5 [33]. Consistently, 7αDH-mediated production of DCA did not induce colonic tumours without AOM/DSS in our study but it increased Ki67+ epithelial cell numbers and enhanced the expression of genes previously shown to be involved in secondary BA-associated colonic tumorigenesis [31,32]. The tumour-promoting role of secondary BAs in susceptible hosts due to diet is also supported by our observation of Western diet-driven increase in Ki67+ cells in the colon of *APC*$^{1311/+}$ pigs. Furthermore, enhanced faecal excretion of BAs by colestyramine was associated with reduced proliferation in the colonic epithelium. This finding provides additional pre-clinical evidence for the potential use of colestyramine for CRC prevention. Previous data in mice showed that colestyramine decreased the expression of genes involved in epithelial cell proliferation in the colon and that it could prevent streptozotocin and high-fat diet-induced hepatocellular carcinoma [33,34]. The use of BA sequestrants in individuals at increased CRC risk appears to be promising for prevention, since pre-diagnostic high plasma levels of BAs were linked to CRC outcome in a prospective study [35]. In this context of preventive BA reduction, it is worth noticing that secondary BAs also increased the expression of genes with tumour-suppressive or essential regulatory functions (e.g., *Guca2a*, *Muc2*, *Pparg*) in our gnotobiotic mice, suggesting that 7αDH-associated microbial metabolites

have a fundamental role in regulating intestinal epithelium homeostasis and regeneration. Thus, low but not completely abolished DCA levels seem to be a promising preventive or therapeutical aim for CRC risk reduction. Recently, BAs were shown to be required for TGR5-dependent regeneration of intestinal epithelial cells and protection from colitis in mice [36], further supporting the importance of physiological BA levels.

In the mouse experiments, we detected a larger caecal BA pool and higher DCA concentrations in female compared to male animals. It is known that female and male mice differ in their BA composition and female mice tend to have higher serum and liver DCA concentrations [37–40]. Moreover, sex hormones influence hepatic BA metabolism, including their production, secretion, and absorption [37,38]. Therefore, our data is in line with already described sex differences in BAs and illustrates the importance to investigate both sexes. Besides BAs, sex hormones also affect CRC risk directly: testosterone increases CRC risk [41,42], whilst oestrogen has the opposite effect [43–45]. This possibly explains why, in our gnotobiotic experiments, colonic tumour numbers were increased by secondary BA production in both male and female mice despite markedly higher DCA concentrations in the latter group.

Besides the causal role of secondary BAs in experimental CRC as demonstrated here, Western diet may promote CRC risk via the microbiome in several manners. For example, a recent study by Yang et al. (2022) [46] demonstrated that experimental CRC was associated with higher levels of *Alistipes* spp. and dysregulation of gut microbial co-metabolism leading to higher levels of glycerophospholipids. Moreover, diets high in fat content are usually associated with increased occurrence of *Enterobacteriaceae*, potentially including pks-expressing *Escherichia coli* with tumorigenic effects [47]. CRC risk does not exclusively arise from the increase in tumour-promoting factors but also from the lack of tumour-suppressive dietary compounds, including complex carbohydrates fermented by gut bacteria to SCFA such as butyrate [8,9,48]. Furthermore, Western or high-fat diets are very diverse in terms of fat content and quality, with consequences regarding effects on the host. A recent study by Dmitrieva-Posocco et al. (2022) [49] showed that a ketogenic diet, highly enriched in fat and very low in carbohydrates, reduced experimental colonic tumorigenesis due to anti-proliferative effects of the ketone body β-hydroxybutyrate. However, the long-term clinical relevance of ketogenic diets remains to

be demonstrated. Taken together, these findings highlight the complexity of diet-associated changes in gut microbial metabolism and support the use of model organisms and experimental diets with detailed composition to unravel the influence of nutrition on CRC development or prevention.

In conclusion, our studies demonstrate the causal role of gut microbial 7αDH activity in experimental CRC. Secondary BAs, in particular DCA, are implicated in the tumour-promoting effects of Western diets, which provides a promising target for CRC prevention via dietary intervention or modulation of gut microbial BA metabolism.

Methods

Animal work

All experiments were carried out according to the German Animal Welfare Act and the European Union Normative for Care and Use of Experimental Animals. Individual approval numbers from the corresponding authorities are provided in the following subsections that describe the specific experiments.

Porcine experiments

These experiments were approved by the Federal Government of Bavaria (permit no. ROB55.2-2-2532.Vet_02-18-33). Pigs were provided by the Chair of Livestock Biotechnology at the Technical University of Munich, Germany, and were housed and sampled at the animal facility Thalhausen (Faculty of Life Science Weihenstephan, Freising, Germany).

Dietary Interventions in *APC*$^{1311/+}$ pigs

The experimental design is depicted in**. Fig. S1**. *APC*$^{1311/+}$ pigs (German landrace × minipig crossbreed) [25] underwent colonoscopy at the age of 3 months to enable their separation into two groups with a comparable distribution of individuals in terms of polyp numbers and size, sex, and littermates. Both groups were fed a standard diet until the dietary intervention started at the age of 4 months to allow for recovery after colonoscopy. The control (CTRL) and experimental diet enriched in red meat and lard (RL) were specifically designed for this experiment and purchased from ssniff Spezialdiäten GmbH (Soest, Germany; cat. no. S5745-S074 and S5745-S076, respectively). Main differences

between the diets are illustrated in **Fig. S1** and their detailed compositions are provided in **Table S1.** The diets were fed to the pigs in a restricted manner (approx. 1 kg/d) for 3 months until the age of 7 months. At the end of the feeding period, faecal samples were taken, and colonoscopy was performed, including biopsy collection. Two RL pigs dropped out of the study due to tumour-independent reasons (meningitis and a foot malformation).

For the second feeding trial testing the effects of colestyramine, the overall experimental design was as in the first experiment (**Fig**. **S1**). However, *APC*$^{1311/+}$ pigs were assigned to three groups instead of two (n = 4-5 pigs each): CTRL, RL, and COL (= RL diet supplemented with 12 g/kg colestyramine; Ratiopharm GmbH, Ulm, Germany; EAN 4150037520609). The recommended dose by the manufacturer is 4-16 g/day for adult subjects. Additional components of the drug colestyramine besides the active agent were added to CTRL and RL diet. Detailed diet compositions are available in **Table S1.**

Colonoscopy

Pigs underwent colonoscopy one month prior to dietary intervention and after the three months of experimental feeding. To reduce the load of faecal material in the large bowel, pigs were fasted for 24 h before the procedure. Based on bodyweight, pigs were narcotised (0.2 mg/kg ketamin and 0.05 mL/kg azaperon) and the large bowel was flushed with tap water to remove remaining luminal content. Tissue biopsies and images were taken using a STORZ colonoscopy system (Flexible SILVER SCOPE®).

Collection of faecal samples and sampling

In both pig trials, fresh faecal samples were collected prior to (4 months of age) and immediately after dietary intervention (7 months of age) before colonoscopy. In brief, faecal material was taken directly from the rectum of each pig using sterile gloves and placed into individual, sterile plastic containers. Solely the material from core areas of the faeces was collected using a sterile spatula. Samples were immediately frozen on dry ice for later sequencing and metabolomics and stored at -80°C. Tissue samples from the rectum were collected either during colonoscopy (pig trial 1) or after the pigs were culled (pig trial 2). The resulting samples were formalin-fixed and paraffin embedded tissue blocks were stored at room temperature.

Mouse experiments

BACOMI consortium

The synthetic microbial community BACOMI (Bile acid-converting microbiota) contains six bacterial species (all obtained from the Leibniz-Institute DSMZ - German Collection of Microorganisms and Cell Cultures, Germany) that can transform the host-derived primary BAs into dehydroxylated secondary BAs (adapted from Ridlon et al. [50]) (**Fig. S1d**). *Bacteroides uniformis* (*B. uniformis*) DSM 6597, *Phocaeicola vulgatus* (*P. vulgatus*) DSM 1447 and *Parabacteroides distasonis* (*P. distasonis*) DSM 20701 express bile salt hydrolases (BSH) that produce free primary BAs from conjugated counterparts. *Bilophila wadsworthia* (*B. wadsworthia*) DSM 11045 can further metabolise taurine released by BSH activity into H_2S. *Clostridium scindens* (*C. scindens*) DSM 5676 is the key-member of the BACOMI consortium, as it is the only species with 7α-dehydroxylating (7αDH) activity. Finally, *Blautia producta* (*B. producta*) DSM 2950 was added due to being a dominant human gut bacterium that is H_2-consuming, acetogenic, able to isomerise bile acids and thus increases variability of the BA pool. The other 7αDHing species *Extibacter muris* (*E. muris*) DSM 28560 was isolated and described by us and available in the in-house collection [51,52]. All bacteria except for *B. wadsworthia* were cultured in brain heart infusion (BHI) medium supplemented with resazurin, hemin, yeast extract and L-cysteine under anaerobic conditions. *B. wadsworthia* was cultured as previously described [53].

Gnotobiotic mouse experiments

The experiments were approved by the Ministry of Social Affairs, Health, Integration and Consumer Protection of the state Brandenburg (permit no. 2347-15-2021). Germfree male and female wildtype mice (BALB/cJ) were kept in positive-pressure isolators at the animal facility of the German Institute for Human Nutrition Potsdam-Rehbruecke (Nuthetal, Germany) with a 12 h light-dark cycle at 22 ± 2 °C and 55 ± 5 % air humidity. Starting 1 week prior to colonization, the mice were switched from standard diet to a high-fat diet (HFD, **Table S1)**. Mice (n = 10 per group) were colonised by gavage (10^8 cells per bacterium in 100 μL medium; 50 μL orally and 50 μL rectally at day 0 and 2) with BACOMI either with (7αDH+) or without (7αDH-) *C. scindens*. After colonisation, mice were either kept for 13 weeks (**Fig. S1 and Fig. 5**) or subjected to further treatment to induce experimental CRC (**Fig. 6)**. In the latter case, mice received three intraperitoneal

injections of azoxymethane (AOM) (5 mg/kg body weight) in the interval of one week, starting at week 2 after colonization. Five days after the final AOM injection, mice were treated with 3 cycles of dextran sodium sulphate (DSS) with 5 days of DSS (1.5 % in drinking water) followed by 16 days of normal drinking water. Mice were culled two weeks after the end of the AOM/DSS treatment and colonic tumours were counted using a binocular microscope. The colonization and AOM/DSS treatment of mice with *E. muris* followed the same protocol, but mice were kept 2 weeks longer after colonization and prior to AOM/DSS treatment to confirm colonization status. For BACOMI with *C. scindens* colonization, three mice (male n = 1, female n = 2) dropped out in the 7αDH+ group during the first DSS cycle, whereas for the 7αDH- group, two mice (male n = 1, female n = 1) dropped out at the end of the third DSS cycle or after the first AOM injection, respectively. For BACOMI with *E. muris* colonization, two female mice dropped out in the 7αDH+ group after the first DSS cycle.

Quantitative real-time PCR for intestinal gene expression

The Dynabeads mRNA purification kit (ThermoFisher Scientific, USA) was used for mRNA isolation. Lysis buffer (200 μl) and 10 zirconium beads were added to approximately 5 mg of intestinal tissue stored at -80 °C in RNA later tissue reagent (Qiagen, Germany). A Tissue lyser (Qiagen, Germany) was then used for homogenisation (2 × 2 min at 50 Hz with a 2 min break in between). The lysate was pulled through a syringe five times with a 1 mL syringe and centrifuged (14,000 rpm, 2 min, room temperature). The rest of the protocol was as per the manufacturer's instructions. mRNA concentrations were determined using a Nanodrop (Peqlab VWR, USA) and 20 ng were used for reverse transcription using the RevertAid H Minus First Strand cDNA Synthesis kit (ThermoFisher Scientific, USA) according to manufacturer's recommendations. For qPCR, the mastermix was prepared according to the manufacturer's recommendations given by the Quantinova SYBR Green PCR Kit (Qiagen, Germany), and forward and reverse primers added (0.5 μM each) (**Table S5**). Then, 4 ng template cDNA was used in a total reaction volume of 10 μl. Samples were amplified using the 7500 Fast Real-Time PCR System (Applied Biosystems, USA). To determine C_T-values, the Life Technologies 7500 Software (version 2.3) was used. Normalization was to the housekeeping gene *Rpl13a,* which encodes for

the 60S ribosomal protein L13a. Results were calculated relative to the control group of 7αDH- mice.

Immunohistochemistry (IHC) and immunofluorescence (IF)

Specimens from the two pig trials were fixed in 4 % formaldehyde solution for 24 h, embedded, and sectioned (3 μm). The tissue sections were then deparaffinised, antigen unmasked (citrate buffer, pH = 6) and endogenous peroxidases were inactivated in 3% H_2O_2 for 10 min. After blocking for 1 h (2% goat serum in PBS), sections were incubated overnight at 4 °C with the primary antibody for Ki67 (Rabbit, DSC innovative Diagnostik-System KI681C002, dilution 1:400) followed by a second overnight incubation with the secondary antibody (Goat Anti-Rabbit IgG, Santa Cruz sc-2780, dilution 1:400). Peroxidase activity was detected using diaminobenzidine (DAB) substrate or the VECTASTAIN® Elite® ABC Kit (Vectorlab PK-6100), respectively. Staining of Ki67 was considered positive and quantified only when detected in nuclei. Ten randomly selected fields (magnification x40) from each tissue section were analysed. Values are presented as the percentage of the stained cells per area.

For the gnotobiotic mouse trial (**Fig. 5**), the dissected tissues were fixed using Methacarn solution and embedded in paraffin. Tissues were cut into 4 μm-thick sections and deparaffinised by heating (60 °C, 15 min) followed by two times xylol for 3 min. The specimens were then rehydrated using a decreasing alcohol series: 100 % for 2 min, 96 % for 2 min, and 70 % for 1 min, followed by water for 1 min. After rinsing twice in water (5 min each), the specimens were boiled in 10 mM citrate buffer (pH = 6) for 30 min for antigen retrieval, followed by 30 min of cooling. Thereafter, the specimens were washed 3 times with water for 5 min, once with PBS for 5 min, and then blocked with PBS containing 5 % goat serum for 1 h at room temperature. Primary antibodies against Ki67 (ab15580, dilution 1:200) were incubated overnight at 4°C. Specimens were then washed three times in PBS (5 min each) and incubated with the secondary antibody (AlexaFluor-488, ThermoFisher, dilution 1:200), and Hoechst (dilution 1:200) for 1-2 h at room temperature. All antibodies were diluted in PBS containing 1 % bovine serum albumin and 0.3 % Triton X-100. Finally, the specimens were washed in PBS for 5 min each and cover with glass slides using mounting medium (Vector Laboratories, United States). For imaging, a confocal laser microscope was used (LSM 780 microscope, Zeiss, Germany).

Tile scans with 40x magnification were acquired and analysed with the ZEN (black edition) 2.3 software (Zeiss, Germany).

Microbiota composition analysis

Metagenomic DNA was obtained using a modified version of a previously published protocol [54,55]. Cells were lysed mechanically via bead-beating and DNA was purified on columns (Macherey-Nagel, Germany). A robotised platform (Biomek4000, Beckman-Coulter, Germany) was then used for library construction. The V3-V4 regions of 16S rRNA genes were amplified (25 cycles) in a two-step PCR [56] using primers 341F (5′-cctacgggnggcwgcag) and 785R (5′-gactachvgggtatctaatcc) [57] and 24 ng of template DNA. A double combinatorial indexing strategy was used. Amplicons were purified using the AMPure XP system (Beckmann Coulter, Germany), pooled in equimolar amounts and sequenced in paired-end mode using a MiSeq system (Illumina).

Raw data were processed using IMNGS (https://www.imngs.org) [58], an online platform based on UPARSE [59]. Sequences were clustered into operational taxonomic units (OTUs) at 97% sequence similarity and only those with a relative abundance ≥ 0.25% in at least one sample were kept to exclude spurious OTUs [60]. Parameters for data processing were: min/max sequence length, 300-500nt; barcode mismatch, 1; end-trim length, 15; max. no. expected errors, 3; trimming q score, 3. The number of sequences per sample after filtering was 26,286 ± 8,044 for the first pig trial and 12,564 ± 3,954 for the gnotobiotic mouse experiment with *E. muris*. Downstream diversity and composition analyses were performed in Rhea (https://github.com/Lagkouvardos/Rhea) [61]. For the first pig trial, taxonomies were assigned using SILVA release 128 [62]. Several families showed a significantly different behaviour between the feeding groups over the time. A pseudocount (lowest value × 10) was added to the normalised relative abundance of each family per sample before calculation to avoid division by zero. For family comparison over time, a start-adjusted delta-value was calculated as follows: (end – start) / start. For changes in α-diversity, original values without pseudo-count were used for the same calculation. Identities of the OTUs for the gnotobiotic mouse experiment were confirmed using Eztaxon [63]. Normalised relative abundances are plotted in **Fig. 2** and **Fig. 6** and provided in **Table S2** and **Table S3.**

For the gnotobiotic mouse trials with *C. scindens,* the QIAmp Fast DNA Stool Mini Kit (Qiagen, Germany) was used to extract and purify DNA from colon content. Approximately 50-80 mg frozen content was added to a cryo-tube containing ca. 100 mg of 0.1 mm glass beads, and 1 mL of InhibitEx buffer, followed by bead-beating (Uniprep, UniEquip, Germany) for 2 × 5 min at 3,000 rpm. All samples were processed according to manufacturer's instructions except for the elution volume (changed to 70 μL). For DNA isolation from bacterial cultures, the Genomic DNA from Microorganisms Kit (Macherey-Nagel, Germany) was used as per the manufacturer's instructions. The disruption time was 12 min, and the samples were eluted twice using the same elution buffer.

A standard curve plotting bacterial cell number against C_T-value was established for each BACOMI species using RT-qPCR and species-specific primers (**Table S5**). The standard curve was generated from overnight bacterial cultures and cell numbers were determined using a Thoma cell counting chamber (Fein-Optik, Germany). For quantification, bacterial DNA was isolated from colon content and bacterial cell numbers (**Table S4**) were calculated using the generated standard curve.

BA measurements

Pig stool samples from trial 1 and 2 were analysed as described previously by Wegner et al. (2017) and Reiter et al. (2021), respectively [64,65].

For the BACOMI mouse experiments with *C. scindens,* lyophilised caecal content (125 mg) were mixed with 450 μL acetonitrile, followed by 15 min vortexing and then centrifugation (13,000 × g, 60 min, 21 °C). Supernatant (300 μL) was mixed with the internal standards (ISTDs) d_4-CDCA and d_4-LCA (10 μM each) and dried in a SpeedVac system (Jouan RC10.22, ThermoFisher Scientific, USA). The residue was dissolved with methanol and water [1:1]. Chromatographic separation of 5 μL sample was achieved on a 1290 Infinity II HPLC (Agilent Technologies, Germany) equipped with a Poroshell EC-C18 column (Agilent Technologies) (3.0 × 150 mm, 2.7 μm) connected to a guard column (3.0 × 5 mm, 2.7 μm) of the same material. The column was tempered to 30 °C. A mobile phase system consisting of 10 mM ammonium acetate/acetonitrile (80:20 v:v; solvent A) and water/acetonitrile (20:80 v:v; solvent B), was applied at a flow rate of 0.2 mL/min. The initial solvent composition of 85% solvent A was maintained for 6 min. Then, solvent A

was decreased stepwise to 70, 40 and 20% within 20, 30 and 40 min of total run-time, respectively. After 45 min, the mobile phase reached initial conditions again. MS/MS analysis was carried out using a 6495C triple-quadrupole mass spectrometer (Agilent Technologies) operating in the negative electrospray ionization mode (ESI-). The ion source parameters were: sheath gas temperature, 400 °C; sheath gas flow, 12 L/min of nitrogen; nebuliser pressure, 40 psi; drying gas temperature, 120 °C; drying gas flow, 15 L/min of nitrogen; capillary voltage, 4500 V; nozzle voltage, 0 V; iFunnel high pressure RF voltage, 90 V and iFunnel low pressure RF voltage, 60 V. A total of 20 compounds (18 bile acids and 2 ISTDs) were simultaneously analysed by single reaction monitoring (SRM) or, if feasible, by multiple reaction monitoring (MRM). HPLC-MS/MS parameters are given in **Table S6.** Quantification was performed using MassHunter Workstation Quantitative Analysis for QQQ (Version 10.1, Agilent Technologies). Analytes were externally calibrated in the concentration range of 0.09 to 90 μM (ISTDs constantly 10 μM). BA concentrations were normalised to dry weight of the caecal content subjected to extraction.

For the gnotobiotic mouse experiment with *E. muris,* samples were lyophilised overnight at –60 °C. The dried caecal contents were weighed, and 6 ceramic beads (2.5 mm) were added to each tube. Proportionally to the weight of each sample, between 500 μL and 1500 μL of MeOH/H_2O (2/1) + 0.1% formic acid was used as extraction solvent. Samples were homogenised in a Precellys 24 Tissue Homogenizer (Bertin Instruments, France) at 6500 rpm 2 x 20” beat and 20” rest. The homogenised caecal samples were centrifuged at 21,000 rcf, for 15 min, at 4 °C. 100uL from each supernatant or calibration standard were transferred into individual wells of 2 mL 96-well plate. 50 μL of an ISTD solution (CA-d_4, CDCA-d_4, TCA-d_4, TUDCA-d_4, DCA-d_4 and LCA-d_4, each at 2 μM in methanol) was pipetted in each well. Immediately after the addition of ISTD, 600 μL of 0.2% formic acid in H_2O was added to each sample or calibration standard level. The 96-well plate was shaken with an orbital shaker at 300 rpm and centrifuged at 3500 rpm, 5 min, 4 °C. The contents of the 96-well plate were extracted by solid phase extraction with an Oasis HLB 96-well uElution plate (Waters, USA). The extracted samples were dried in a Biotage® SPE Dry 96 (Biotage, Sweden) at 20 °C and reconstituted with 100 μL of MeOH/H_2O

(50/50). The plate was shaken with an orbital shaker at 300 rpm, 5 min and centrifuged at 3500 rpm, 5 min, 4 °C. The samples were injected on the LC-HRMS system.

The quantitative method was performed on an Agilent ultrahigh-performance liquid chromatography 1290 series coupled in tandem to an Agilent 6530 Accurate-Mass Q-TOF mass spectrometer [66]. The separation was done on a Zorbax Eclipse Plus C18 column (2.1 × 100 mm, 1.8 μm) and a guard column Zorbax Eclipse Plus C18 (2.1 × 5 mm, 1.8 µm), both provided by Agilent technologies (USA). The column compartment was kept heated at 50 °C. Two different solutions were used as eluents: ammonium acetate [5 mM] in water as mobile phase A and pure acetonitrile as mobile phase B. A constant flow of 0.4 mL/min was maintained over 26 min of run time with the following gradient (expressed in eluent B percentage): 0-5.5 min, constant 21.5% B; 5.5-6 min, 21.5-24.5% B; 6-10 min, 24.5-25% B; 10-10.5 min, 25-29% B; 10.5-14.5 min, isocratic 29% B; 14.5-15 min, 29-40% B; 15-18 min, 40-45% B; 18-20.5 min, 45-95% B; 20.5-23 min, constant 95% B; 23-23.1 min, 95-21.5% B; 23.10-26 min, isocratic 21.50% B. The system equilibration was implemented at the end of the gradient for 3 min in initial conditions. The autosampler temperature was maintained at 10 °C and the injection volume was 5 μL. The ionisation mode was operated in negative mode for the detection using the Dual AJS Jet stream ESI Assembly. The QTOF acquisition settings were configured in 4 GHz high-resolution mode (resolution 17000 FWHM at m/z 1000), data storage in profile mode and the high-resolution full MS chromatograms were acquired over the range of m/z 100-1700 at a rate of 3 spectra/s. The mass spectrometer was calibrated in negative mode using ESI-L solution from Agilent technologies every 6 h to maintain the best possible mass accuracy. Source parameters were setup as follows: drying gas flow, 8 L/min; gas temperature, 300 °C; nebuliser pressure, 35 psi; capillary voltage, 3500 V; nozzle voltage, 1000 V. Data were processed afterwards using the MassHunter Quantitative software and MassHunter Qualitative software (Agilent technologies, USA) to control the mass accuracy for each run. In the quantitative method, 43 bile acids were quantified by calibration curves. The quantification was corrected by addition of internal standards in all samples and calibration levels. Extracted ion chromatograms were generated using a retention time window of ± 1.5 min and a mass extraction window of ± 60ppm around the theoretical mass of the targeted bile acid.

For all experiments, BAs that were not detected by the respective methods were assumed to absent, set to 0 μmol/g and only those BAs detected in at least 50 % of the animals in at least one group were considered for downstream analyses. Statistics were done only on dominant BA species (the concentration thresholds are shown in the figures; all individual values for all BAs are available in **Table S2-4**). UDCA is a primary BA in rodents, but a secondary BA in humans [67,68]. Due to their similarity to humans, we classified UDCA as a secondary BA in pigs.

Lipidomic analyses

Faecal homogenates for analysis of fatty acids, sterols and stanols were prepared in isopropanol as described before [69]. Subsequently, the homogenates were used for both fatty acid and sterol/stanol analysis. Concentrations of total faecal fatty acids were determined by gas chromatography coupled to mass spectrometry (GC-MS) as described previously [70] with some modifications. Samples were derivatised to fatty acid methyl ester (FAME). The initial column temperature of 50 °C was held for 0.75 min, increased with 40 °C/min to 110 °C, with 6 °C/min to 210 °C, with 15 °C/min to 250 °C and held for 2 min. Iso- and anteiso-FAMEs standards were applied to identify branched chain fatty acids and to calibrate the instrument response. Samples for analysis of sterols and stanols were analysed as described previously [71].

Data visualisation and statistics

Statistical analyses were done using R (Version 4.2.1) [72] in RStudio [73] using the rstatix package. For microbiota analyses, detailed information is provided in Rhea (https://github.com/Lagkouvardos/Rhea) [61]. Comparisons between two groups were done by Wilcoxon tests and Benjamini-Hochberg adjustment. Comparisons between three groups were done by Kruskal Wallis tests with Dunn's multiple comparisons and Benjamini-Hochberg adjustments. Adjusted p-values are with stars as defined in the corresponding legends; non-adjusted p-values are given as numbers directly in the graphs whenever appropriate. All graphs were created in R using tidyverse (ggplot2; RRID:SCR_014601) [74], ggpubr, cowplot, and ggbreak [75].

Data availability

All data used to generate the figures is available in the supplementary tables (**Table S2-4**). Raw data of the 16S rRNA gene amplicon sequencing were submitted to ENA and are available under project PRJEB60380.

Acknowledgements

We are grateful to Viola and Steffen Loebnitz, Tatiana Flisikowska, and Thomas Winogrodzky from the Chair of Livestock Biotechnology at the Technical University of Munich, Germany, for their support with pig experiments. We also thank Ines Grüner, Anika Sander, Sabine Schmidt and Anke Gühler from the German Institute of Human Nutrition Potsdam-Rehbruecke, Nuthetal, Germany, for their help with the germfree mouse colony and colonization experiments, and Tobias Goris and Annett Braune for their critical review of data.

Funding

TC received funding from the German Research Foundation (DFG): project no. 460129525, NFDI4Microbiota; project no. 395357507, SFB1371; project no. CL481/8-1. TC and KF received funding from the German Ministry for Research and Education (BMBF): consortium project Mi-EOCRC (KZ. 01KD2102D). SO received funding from the German Research Foundation (DFG): project no. 338582098.

References

1. Sung, H., Ferlay, J., Siegel, R. L., Laversanne, M., Soerjomataram, I., Jemal, A. & Bray, F. Global Cancer Statistics 2020: GLOBOCAN Estimates of Incidence and Mortality Worldwide for 36 Cancers in 185 Countries. *CA. Cancer J. Clin.* **71**, 209–249 (2021).

2. Lichtenstein, P., Holm, N. V., Verkasalo, P. K., Iliadou, A., Kaprio, J., Koskenvuo, M., Pukkala, E., Skytthe, A. & Hemminki, K. Environmental and heritable factors in the causation of cancer--analyses of cohorts of twins from Sweden, Denmark, and Finland. *N. Engl. J. Med.* **343**, 78–85 (2000).

3. Huxley, R. R., Ansary-Moghaddam, A., Clifton, P., Czernichow, S., Parr, C. L. & Woodward, M. The impact of dietary and lifestyle risk factors on risk of colorectal cancer: A quantitative overview of the epidemiological evidence. *Int. J. Cancer* **125**, 171–180 (2009).

4. Keum, N. N. & Giovannucci, E. Global burden of colorectal cancer: emerging trends, risk factors and prevention strategies. *Nat. Rev. Gastroenterol. Hepatol.* **16**, 713–732 (2019).

5. Reynolds, A., Mann, J., Cummings, J., Winter, N., Mete, E. & Te Morenga, L. Carbohydrate quality and human health: a series of systematic reviews and meta-analyses. *Lancet* **393**, 434–445 (2019).

6. Garcia-Larsen, V., Morton, V., Norat, T., Moreira, A., Potts, J. F., Reeves, T. & Bakolis, I. Dietary patterns derived from principal component analysis (PCA) and risk of colorectal cancer: a systematic review and meta-analysis. *Eur. J. Clin. Nutr.* **73**, 366–386 (2019).

7. Chen, H. M., Yu, Y. N., Wang, J. L., Lin, Y. W., Kong, X., Yang, C. Q., Yang, L., Liu, Z. J., Yuan, Y. Z., Liu, F., Wu, J. X., Zhong, L., Fang, D. C., Zou, W. & Fang, J. Y. Decreased dietary fiber intake and structural alteration of gut microbiota in patients with advanced colorectal adenoma. *Am. J. Clin. Nutr.* **97**, 1044–1052 (2013).

8. O'Keefe, S. J. D., Li, J. V., Lahti, L., Ou, J., Carbonero, F., Mohammed, K.,

Posma, J. M., Kinross, J., Wahl, E., Ruder, E., Vipperla, K., Naidoo, V., Mtshali, L., Tims, S., Puylaert, P. G. B., Delany, J., Krasinskas, A., Benefiel, A. C., Kaseb, H. O., Newton, K., Nicholson, J. K., De Vos, W. M., Gaskins, H. R. & Zoetendal, E. G. Fat, fibre and cancer risk in African Americans and rural Africans. *Nat. Commun.* **6**, 1–29 (2015).

9. Ocvirk, S., Wilson, A. S., Posma, J. M., Li, J. V., Koller, K. R., Day, G. M., Flanagan, C. A., Otto, J. E., Sacco, P. E., Sacco, F. D., Sapp, F. R., Wilson, A. S., Newton, K., Brouard, F., Delany, J. P., Behnning, M., Appolonia, C. N., Soni, D., Bhatti, F., Methé, B., Fitch, A., Morris, A., Gaskins, H. R., Kinross, J., Nicholson, J. K., Thomas, T. K. & O'Keefe, S. J. D. A prospective cohort analysis of gut microbial co-metabolism in Alaska Native and rural African people at high and low risk of colorectal cancer. *Am. J. Clin. Nutr.* **111**, 406–419 (2020).

10. Hill, M. J., Drasar, B. S., Williams, R. E. O., Meade, T. W., Cox, A. G., Simpson, J. E. P. & Morson, B. C. Faecal Bile-Acids and Clostridia in Patients With Cancer of the Large Bowel. *Lancet* **305**, 535–539 (1975).

11. Kawano, A., Ishikawa, H., Kamano, T., Kanoh, M., Sakamoto, K., Nakamura, T., Otani, T., Sakai, T. & Kono, K. Significance of fecal deoxycholic acid concentration for colorectal tumor enlargement. *Asian Pacific J. Cancer Prev.* **11**, 1541–1546 (2010).

12. Ocvirk, S. & O'Keefe, S. J. D. Dietary fat, bile acid metabolism and colorectal cancer. *Semin. Cancer Biol.* **73**, 347–355 (2021).

13. Ou, J., Carbonero, F., Zoetendal, E. G., DeLany, J. P., Wang, M., Newton, K., Gaskins, H. R. & O'Keefe, S. J. Diet, microbiota, and microbial metabolites in colon cancer risk in rural Africans and African Americans. *Am. J. Clin. Nutr.* **98**, 111–120 (2013).

14. Wirbel, J., Pyl, P. T., Kartal, E., Zych, K., Kashani, A., Milanese, A., Fleck, J. S., Voigt, A. Y., Palleja, A., Ponnudurai, R., Sunagawa, S., Coelho, L. P., Schrotz-King, P., Vogtmann, E., Habermann, N., Niméus, E., Thomas, A. M., Manghi, P., Gandini, S., Serrano, D., Mizutani, S., Shiroma, H., Shiba, S., Shibata, T.,

Yachida, S., Yamada, T., Waldron, L., Naccarati, A., Segata, N., Sinha, R., Ulrich, C. M., Brenner, H., Arumugam, M., Bork, P. & Zeller, G. Meta-analysis of fecal metagenomes reveals global microbial signatures that are specific for colorectal cancer. *Nat. Med.* **25**, 679–689 (2019).

15. Wang, S., Dong, W., Liu, L., Xu, M., Wang, Y., Liu, T., Zhang, Y., Wang, B. & Cao, H. Interplay between bile acids and the gut microbiota promotes intestinal carcinogenesis. *Mol. Carcinog.* **58**, 1–13 (2019).

16. Bernstein, C., Holubec, H., Bhattacharyya, A. K., Nguyen, H., Payne, C. M., Zaitlin, B. & Bernstein, H. Carcinogenicity of deoxycholate, a secondary bile acid. *Arch. Toxicol.* **85**, 863–871 (2011).

17. Flynn, C., Montrose, D. C., Swank, D. L., Masako, N., Ilsley, J. N. M. & Rosenberg, D. W. Deoxycholic Acid Promotes the Growth of Colonic Aberrant Crypt Foci. *Mol. Carcinog.* **46**, 60–70 (2007).

18. Cao, H., Luo, S., Xu, M., Zhang, Y., Song, S., Wang, S., Kong, X., He, N., Cao, X., Yan, F. & Wang, B. The secondary bile acid, deoxycholate accelerates intestinal adenoma–adenocarcinoma sequence in *Apc*$^{min/+}$ mice through enhancing Wnt signaling. *Fam. Cancer* **13**, 563–571 (2014).

19. Cao, H., Xu, M., Dong, W., Deng, B., Wang, S., Zhang, Y., Wang, S., Luo, S., Wang, W., Qi, Y., Gao, J., Cao, X., Yan, F. & Wang, B. Secondary bile acid-induced dysbiosis promotes intestinal carcinogenesis. *Int. J. Cancer* **140**, 2545–2556 (2017).

20. Moser, A. R., Pitot, H. C. & Dove, W. F. A Dominant Mutation That Predisposes to Multiple Intestinal Neoplasia in the Mouse. *Science* **247**, 322–324 (1990).

21. Moser, A. ., Luongo, C., Gould, K. ., McNeley, M. ., Shoemaker, A. . & Dove, W. . *Apc*^{Min}: A mouse model for intestinal and mammary tumorigenesis. *Eur. J. Cancer* **31**, 1061–1064 (1995).

22. Gonzalez, L. M., Moeser, A. J. & Blikslager, A. T. Porcine models of digestive disease: The future of large animal translational research. *Transl. Res.* **166**, 12–27

(2015).

23. Rose, E. C., Blikslager, A. T. & Ziegler, A. L. Porcine Models of the Intestinal Microbiota: The Translational Key to Understanding How Gut Commensals Contribute to Gastrointestinal Disease. *Front. Vet. Sci.* **9**, 1–8 (2022).

24. Flisikowska, T., Merkl, C., Landmann, M., Eser, S., Rezaei, N., Cui, X., Kurome, M., Zakhartchenko, V., Kessler, B., Wieland, H., Rottmann, O., Schmid, R. M., Schneider, G., Kind, A., Wolf, E., Saur, D. & Schnieke, A. A porcine model of familial adenomatous polyposis. *Gastroenterology* **143**, 1173-1175.e7 (2012).

25. Flisikowski, K., Perleberg, C., Niu, G., Winogrodzki, T., Bak, A., Liang, W., Grodziecki, A., Zhang, Y., Pausch, H., Flisikowska, T., Klinger, B., Perkowska, A., Kind, A., Switonski, M., Janssen, K. P., Saur, D. & Schnieke, A. Wild-type APC Influences the Severity of Familial Adenomatous Polyposis. *Cmgh* **13**, 669-671.e3 (2022).

26. Song, M., Yang, Q., Zhang, F., Chen, L., Su, H., Yang, X., He, H., Liu, F., Zheng, J., Ling, M., Lai, X., Zhu, X., Wang, L., Gao, P., Shu, G., Jiang, Q. & Wang, S. Hyodeoxycholic acid (HDCA) suppresses intestinal epithelial cell proliferation through FXR-PI3K/AKT pathway, accompanied by alteration of bile acids metabolism profiles induced by gut bacteria. *FASEB J.* **34**, 7103–7117 (2020).

27. Zarras, P. & Vogl, O. Polycationic salts as bile acid sequestering agents. *Prog. Polym. Sci.* **24**, 485–516 (1999).

28. Streidl, T., Kumar, N., Suarez, L. N., Rohn, S. & Clavel, T. *Extibacter*. in *Bergey's Manual of Systematics of Archaea and Bacteria* 1–7 (Wiley, 2019).

29. Afrizal, A., Jennings, S. A., Hitch, T. C., Riedel, T., Basic, M., Panyot, A., Treichel, N., Hager, F. T., Wong, E. O.-Y., Wolter, B., Viehof, A., von Strempel, A., Eberl, C., Buhl, E. M., Abt, B., Bleich, A., Tolba, R., Blank, L. M., Navarre, W. W., Kiessling, F., Horz, H.-P., Torow, N., Cerovic, V., Stecher, B., Strowig, T., Overmann, J. & Clavel, T. Enhanced cultured diversity of the mouse gut microbiota enables custom-made synthetic communities. *Cell Host Microbe* **30**, 1630-1645.e25 (2022).

30. Farhana, L., Nangia-Makker, P., Arbit, E., Shango, K., Sarkar, S., Mahmud, H., Hadden, T., Yu, Y. & Majumdar, A. P. N. Bile acid: a potential inducer of colon cancer stem cells. *Stem Cell Res. Ther.* **7**, 181 (2016).

31. Pai, R., Tarnawski, A. S. & Tran, T. Deoxycholic Acid Activates β-Catenin Signaling Pathway and Increases Colon Cell Cancer Growth and Invasiveness. *Mol. Biol. Cell* **15**, 2156–2163 (2004).

32. Fu, T., Coulter, S., Yoshihara, E., Oh, T. G., Fang, S., Cayabyab, F., Zhu, Q., Zhang, T., Leblanc, M., Liu, S., He, M., Waizenegger, W., Gasser, E., Schnabl, B., Atkins, A. R., Yu, R. T., Knight, R., Liddle, C., Downes, M. & Evans, R. M. FXR Regulates Intestinal Cancer Stem Cell Proliferation. *Cell* **176**, 1098-1112.e18 (2019).

33. Li, J.-Y., Gillilland, M., Lee, A. A., Wu, X., Zhou, S.-Y. & Owyang, C. Secondary bile acids mediate high-fat diet-induced upregulation of R-spondin 3 and intestinal epithelial proliferation. *JCI insight* **7**, 1–17 (2022).

34. Xie, G., Wang, X., Huang, F., Zhao, A., Chen, W., Yan, J., Zhang, Y., Lei, S., Ge, K., Zheng, X., Liu, J., Su, M., Liu, P. & Jia, W. Dysregulated hepatic bile acids collaboratively promote liver carcinogenesis. *Int. J. Cancer* **139**, 1764–1775 (2016).

35. Kühn, T., Stepien, M., López-Nogueroles, M., Damms-Machado, A., Sookthai, D., Johnson, T., Roca, M., Hüsing, A., Maldonado, S. G., Cross, A. J., Murphy, N., Freisling, H., Rinaldi, S., Scalbert, A., Fedirko, V., Severi, G., Boutron-Ruault, M.-C., Mancini, F. R., Sowah, S. A., Boeing, H., Jakszyn, P., Sánchez, M. J., Merino, S., Colorado-Yohar, S., Barricarte, A., Khaw, K. T., Schmidt, J. A., Perez-Cornago, A., Trichopoulou, A., Karakatsani, A., Thriskos, P., Palli, D., Agnoli, C., Tumino, R., Sacerdote, C., Panico, S., Bueno-de-Mesquita, B., van Gils, C. H., Heath, A. K., Gunter, M. J., Riboli, E., Lahoz, A., Jenab, M. & Kaaks, R. Prediagnostic Plasma Bile Acid Levels and Colon Cancer Risk: A Prospective Study. *JNCI J. Natl. Cancer Inst.* **112**, 516–524 (2020).

36. Sorrentino, G., Perino, A., Yildiz, E., El Alam, G., Bou Sleiman, M., Gioiello, A.,

Pellicciari, R. & Schoonjans, K. Bile Acids Signal via TGR5 to Activate Intestinal Stem Cells and Epithelial Regeneration. *Gastroenterology* **159**, 956-968.e8 (2020).

37. Phelps, T., Snyder, E., Rodriguez, E., Child, H. & Harvey, P. The influence of biological sex and sex hormones on bile acid synthesis and cholesterol homeostasis. *Biol. Sex Differ.* **10**, 1–12 (2019).

38. Fu, Z. D., Csanaky, I. L. & Klaassen, C. D. Gender-divergent profile of bile acid homeostasis during aging of mice. *PLoS One* **7**, 1–13 (2012).

39. Ma, J., Hong, Y., Zheng, N., Xie, G., Lyu, Y., Gu, Y., Xi, C., Chen, L., Wu, G., Li, Y., Tao, X., Zhong, J., Huang, Z., Wu, W., Yuan, L., Lin, M., Lu, X., Zhang, W., Jia, W., Sheng, L. & Li, H. Gut microbiota remodeling reverses aging-associated inflammation and dysregulation of systemic bile acid homeostasis in mice sex-specifically. *Gut Microbes* **11**, 1450–1474 (2020).

40. Selwyn, F. P., Csanaky, I. L., Zhang, Y. & Klaassen, C. D. Special section on drug metabolism and the microbiome: Importance of large intestine in regulating bile acids and glucagon-like peptide-1 in germ-free mice. *Drug Metab. Dispos.* **43**, 1544–1556 (2015).

41. Song, C.-H., Kim, N., Nam, R. H., Choi, S. I., Yu, J. E., Nho, H., Shin, E., Lee, H.-N. & Surh, Y.-J. Testosterone strongly enhances azoxymethane/dextran sulfate sodium-induced colorectal cancer development in C57BL/6 mice. *Am J Cancer Res* **11**, 3145–3162 (2021).

42. Amos-Landgraf, J. M., Heijmans, J., Wielenga, M. C. B., Dunkin, E., Krentz, K. J., Clipson, L., Ederveen, A. G., Groothuis, P. G., Mosselman, S., Muncan, V., Hommes, D. W., Shedlovsky, A., Dove, W. F. & Van Den Brink, G. R. Sex disparity in colonic adenomagenesis involves promotion by male hormones, not protection by female hormones. *Proc. Natl. Acad. Sci. U. S. A.* **111**, 16514–16519 (2014).

43. Son, H. J., Sohn, S. H., Kim, N., Lee, H. N., Lee, S. M., Nam, R. H., Park, J. H., Song, C. H., Shin, E., Na, H. Y., Kim, J. S., Lee, D. H. & Surh, Y. J. Effect of

estradiol in an azoxymethane/dextran sulfate sodium-treated mouse model of colorectal cancer: Implication for sex difference in colorectal cancer development. *Cancer Res. Treat.* **51**, 632–648 (2019).

44. Chlebowski, R. T., Wactawski-Wende, J., Ritenbaugh, C., Hubbell, F. A., Ascensao, J., Rodabough, R. J., Rosenberg, C. A., Taylor, V. M., Harris, R., Chen, C., Adams-Campbell, L. L. & White, E. Estrogen plus Progestin and Colorectal Cancer in Postmenopausal Women. *N. Engl. J. Med.* **350**, 991–1004 (2004).

45. Murphy, N., Strickler, H. D., Stanczyk, F. Z., Xue, X., Wassertheil-Smoller, S., Rohan, T. E., Ho, G. Y. F., Anderson, G. L., Potter, J. D. & Gunter, M. J. A Prospective Evaluation of Endogenous Sex Hormone Levels and Colorectal Cancer Risk in Postmenopausal Women. *J. Natl. Cancer Inst.* **107**, 1–10 (2015).

46. Yang, J., Wei, H., Zhou, Y., Szeto, C.-H., Li, C., Lin, Y., Coker, O. O., Lau, H. C. H., Chan, A. W. H., Sung, J. J. Y. & Yu, J. High-Fat Diet Promotes Colorectal Tumorigenesis Through Modulating Gut Microbiota and Metabolites. *Gastroenterology* **162**, 135-149.e2 (2022).

47. Arthur, J. C., Perez-Chanona, E., Mühlbauer, M., Tomkovich, S., Uronis, J. M., Fan, T.-J., Campbell, B. J., Abujamel, T., Dogan, B., Rogers, A. B., Rhodes, J. M., Stintzi, A., Simpson, K. W., Hansen, J. J., Keku, T. O., Fodor, A. A. & Jobin, C. Intestinal Inflammation Targets Cancer-Inducing Activity of the Microbiota. *Science* **338**, 120–123 (2012).

48. Donohoe, D. R., Holley, D., Collins, L. B., Montgomery, S. A., Whitmore, A. C., Hillhouse, A., Curry, K. P., Renner, S. W., Greenwalt, A., Ryan, E. P., Godfrey, V., Heise, M. T., Threadgill, D. S., Han, A., Swenberg, J. A., Threadgill, D. W. & Bultman, S. J. A gnotobiotic mouse model demonstrates that dietary fiber protects against colorectal tumorigenesis in a microbiota- and butyrate-dependent manner. *Cancer Discov.* **4**, 1387–1397 (2014).

49. Dmitrieva-Posocco, O., Wong, A. C., Lundgren, P., Golos, A. M., Descamps, H. C., Dohnalová, L., Cramer, Z., Tian, Y., Yueh, B., Eskiocak, O., Egervari, G., Lan, Y., Liu, J., Fan, J., Kim, J., Madhu, B., Schneider, K. M., Khoziainova, S.,

Andreeva, N., Wang, Q., Li, N., Furth, E. E., Bailis, W., Kelsen, J. R., Hamilton, K. E., Kaestner, K. H., Berger, S. L., Epstein, J. A., Jain, R., Li, M., Beyaz, S., Lengner, C. J., Katona, B. W., Grivennikov, S. I., Thaiss, C. A. & Levy, M. β-Hydroxybutyrate suppresses colorectal cancer. *Nature* **605**, 160–165 (2022).

50. Ridlon, J. M., Devendran, S., Alves, J. M., Doden, H., Wolf, P. G., Pereira, G. V., Ly, L., Volland, A., Takei, H., Nittono, H., Murai, T., Kurosawa, T., Chlipala, G. E., Green, S. J., Hernandez, A. G., Fields, C. J., Wright, C. L., Kakiyama, G., Cann, I., Kashyap, P., McCracken, V. & Gaskins, H. R. The '*in vivo* lifestyle' of bile acid 7α-dehydroxylating bacteria: comparative genomics, metatranscriptomic, and bile acid metabolomics analysis of a defined microbial community in gnotobiotic mice. *Gut Microbes* **11**, 381–404 (2020).

51. Lagkouvardos, I., Pukall, R., Abt, B., Foesel, B. U., Meier-Kolthoff, J. P., Kumar, N., Bresciani, A., Martínez, I., Just, S., Ziegler, C., Brugiroux, S., Garzetti, D., Wenning, M., Bui, T. P. N. N., Wang, J., Hugenholtz, F., Plugge, C. M., Peterson, D. A., Hornef, M. W., Baines, J. F., Smidt, H., Walter, J., Kristiansen, K., Nielsen, H. B., Haller, D., Overmann, J., Stecher, B. & Clavel, T. The Mouse Intestinal Bacterial Collection (miBC) provides host-specific insight into cultured diversity and functional potential of the gut microbiota. *Nat. Microbiol.* **1**, 1 (2016).

52. Streidl, T., Karkossa, I., Segura Muñoz, R. R., Eberl, C., Zaufel, A., Plagge, J., Schmaltz, R., Schubert, K., Basic, M., Schneider, K. M., Afify, M., Trautwein, C., Tolba, R., Stecher, B., Doden, H. L., Ridlon, J. M., Ecker, J., Moustafa, T., von Bergen, M., Ramer-Tait, A. E. & Clavel, T. The gut bacterium Extibacter muris produces secondary bile acids and influences liver physiology in gnotobiotic mice. *Gut Microbes* **13**, 1–21 (2021).

53. Burkhardt, W., Rausch, T., Klopfleisch, R., Blaut, M. & Braune, A. Impact of dietary sulfolipid-derived sulfoquinovose on gut microbiota composition and inflammatory status of colitis-prone interleukin-10-deficient mice. *Int. J. Med. Microbiol.* **311**, 151494 (2021).

54. Godon, J. J., Zumstein, E., Dabert, P., Habouzit, F. & Moletta, R. Molecular microbial diversity of an anaerobic digestor as determined by small-subunit rDNA

sequence analysis. *Appl. Environ. Microbiol.* **63**, 2802–2813 (1997).

55. Just, S., Mondot, S., Ecker, J., Wegner, K., Rath, E., Gau, L., Streidl, T., Hery-Arnaud, G., Schmidt, S., Lesker, T. R., Bieth, V., Dunkel, A., Strowig, T., Hofmann, T., Haller, D., Liebisch, G., Gérard, P., Rohn, S., Lepage, P. & Clavel, T. The gut microbiota drives the impact of bile acids and fat source in diet on mouse metabolism. *Microbiome* **6**, 1–18 (2018).

56. Berry, D., Mahfoudh, K. Ben, Wagner, M. & Loy, A. Barcoded primers used in multiplex amplicon pyrosequencing bias amplification. *Appl. Environ. Microbiol.* **77**, 7846–7849 (2011).

57. Klindworth, A., Pruesse, E., Schweer, T., Peplies, J., Quast, C., Horn, M. & Glöckner, F. O. Evaluation of general 16S ribosomal RNA gene PCR primers for classical and next-generation sequencing-based diversity studies. *Nucleic Acids Res.* **41**, 1–11 (2013).

58. Lagkouvardos, I., Joseph, D., Kapfhammer, M., Giritli, S., Horn, M., Haller, D. & Clavel, T. IMNGS: A comprehensive open resource of processed 16S rRNA microbial profiles for ecology and diversity studies. *Sci. Rep.* **6**, 1–9 (2016).

59. Edgar, R. C. UPARSE: Highly accurate OTU sequences from microbial amplicon reads. *Nat. Methods* **10**, 996–998 (2013).

60. Reitmeier, S., Hitch, T. C. A., Treichel, N., Fikas, N., Hausmann, B., Ramer-Tait, A. E., Neuhaus, K., Berry, D., Haller, D., Lagkouvardos, I. & Clavel, T. Handling of spurious sequences affects the outcome of high-throughput 16S rRNA gene amplicon profiling. *ISME Commun.* **1**, (2021).

61. Lagkouvardos, I., Fischer, S., Kumar, N. & Clavel, T. Rhea: A transparent and modular R pipeline for microbial profiling based on 16S rRNA gene amplicons. *PeerJ* **5:e2836**, (2017).

62. Pruesse, E., Peplies, J. & Glöckner, F. O. SINA: Accurate high-throughput multiple sequence alignment of ribosomal RNA genes. *Bioinformatics* **28**, 1823–1829 (2012).

63. Yoon, S. H., Ha, S. M., Kwon, S., Lim, J., Kim, Y., Seo, H. & Chun, J. Introducing EzBioCloud: A taxonomically united database of 16S rRNA gene sequences and whole-genome assemblies. *Int. J. Syst. Evol. Microbiol.* **67**, 1613–1617 (2017).

64. Wegner, K., Just, S., Gau, L., Mueller, H., Gérard, P., Lepage, P., Clavel, T. & Rohn, S. Rapid analysis of bile acids in different biological matrices using LC-ESI-MS/MS for the investigation of bile acid transformation by mammalian gut bacteria. *Anal. Bioanal. Chem.* **409**, 1231–1245 (2017).

65. Reiter, S., Dunkel, A., Metwaly, A., Panes, J., Salas, A., Haller, D. & Hofmann, T. Development of a Highly Sensitive Ultra-High-Performance Liquid Chromatography Coupled to Electrospray Ionization Tandem Mass Spectrometry Quantitation Method for Fecal Bile Acids and Application on Crohn's Disease Studies. *J. Agric. Food Chem.* **69**, 5238–5251 (2021).

66. Vico-Oton, E., Volet, C., Jacquemin, N., Lederballe Meibom, K. & Bernier-Latmani, R. Strain-dependent induction of primary bile acid 7-dehydroxylation by cholic acid. *bioRxiv* (2022).

67. Honda, A., Miyazaki, T., Iwamoto, J., Hirayama, T., Morishita, Y., Monma, T., Ueda, H., Mizuno, S., Sugiyama, F., Takahashi, S. & Ikegami, T. Regulation of bile acid metabolism in mouse models with hydrophobic bile acid composition. *J. Lipid Res.* **61**, 54–69 (2020).

68. Li, J. & Dawson, P. A. Animal models to study bile acid metabolism. *Biochim. Biophys. Acta - Mol. Basis Dis.* **1865**, 895–911 (2019).

69. Schött, H. F., Krautbauer, S., Höring, M., Liebisch, G. & Matysik, S. A Validated, Fast Method for Quantification of Sterols and Gut Microbiome Derived 5α/β-Stanols in Human Feces by Isotope Dilution LC-High-Resolution MS. *Anal. Chem.* **90**, 8487–8494 (2018).

70. Ecker, J., Scherer, M., Schmitz, G. & Liebisch, G. A rapid GC-MS method for quantification of positional and geometric isomers of fatty acid methyl esters. *J. Chromatogr. B Anal. Technol. Biomed. Life Sci.* **897**, 98–104 (2012).

71. Kunz, S. & Matysik, S. A comprehensive method to determine sterol species in human faeces by GC-triple quadrupole MS. *J. Steroid Biochem. Mol. Biol.* **190**, 99–103 (2019).

72. R Core Team. R: A Language and Environment for Statistical Computing. at https://www.r-project.org/ (2022).

73. Posit team. RStudio: Integrated Development for R. at http://www.posit.co/ (2022).

74. Wickham H. ggplot2: Elegant Graphics for Data Analysis. at https://ggplot2.tidyverse.org (2016).

75. Xu, S., Chen, M., Feng, T., Zhan, L., Zhou, L. & Yu, G. Use ggbreak to Effectively Utilize Plotting Space to Deal With Large Datasets and Outliers. *Front. Genet.* **12**, 1–7 (2021).

Figure Legends

Fig 1. Effects of Western diet on disease phenotype. **a,** number and size of polyps in the distal colon of *APC*$^{1311/+}$ pigs aged 3 months (3m, 1 month prior to the feeding intervention) or 7 months (7m, end of feeding intervention) and fed either the red meat and lard diet (RL, n = 8; red symbols) or the control diet (CTRL, n = 9; blue). Litters are indicated by different symbols. Lower panel: Exemplary endoscopic pictures (last 40 cm of the colon). **b,** Percentage of Ki67+ cells in crypts of the distal colon from CTRL and RL pigs (n = 3 each) after the feeding intervention; for each pig, 10 randomly selected fields were counted (small coloured dots). Mean values and standard deviations per pig are shown in grey. Lower panel: Exemplary Ki67 staining of distal colon samples. Black bars on the pictures represent 200 μm. Statistics: **a,** Paired Wilcoxon signed rank test; **b,** unpaired Wilcoxon rank sum test.

Fig. 2 Effects of Western diet on faecal microbiota (16S rRNA amplicon sequencing) and bile acids (LC-MS/MS). a, Richness and Shannon effective counts over time (p = 0.0206 and 0.1390, respectively). 4m (4 months) is the start of the dietary intervention, 7m (7 months) the end. **b,** *Beta*-diversity shown as metaNMDS plot of generalised Unifrac distances (p = 0.001, PERMANOVA; pairwise comparisons with Benjamini-Hochberg adjustment: start, p.adj. = 0.399, end, p.adj. = 0.0015). **c,** Relative abundances of dominant bacterial families with significantly different changes over time (end-start/start) between feeding groups (Wilcoxon rank sum test, p ≤ 0.05); **d,** Primary (grey stack bars) and secondary (brown) BA levels in faeces at the end of the feeding period; mean values per feeding group are shown (n = 9 for CTRL, n = 8 for RL). All values are available in **Table S2**. GCA = Glycocholic acid, CDCA = chenodeoxycholic acid, GCDCA= Glycochenodeoxycholic acid, βMCA = β-muricholic acid, CA = cholic acid, HCA = hyocholic acid, TCDCA = tauro-chenodeoxycholic acid, DCA = deoxycholic acid, DHCA = dehydro-lithocholic acid, HDCA= hyo-deoxycolic acid, ωMCA = ω-muricholic acid, 12-KLCA = 12-keto-litocholic acid, 3-DHCA = 3-dehydro cholic acid. **e,** Dot plots of the secondary BAs DCA and 12-KLCA in faeces. Mean values and standard deviations across all pigs per group are shown in grey. Statistics: **d** and **e,** Wilcoxon rank sum test with Benjamini-Hochberg adjustment (* p.adj. ≤ 0.05, ** p.adj. ≤ 0.01).

Fig. 3 Colestyramine treatment in transgenic *APC*$^{1311/+}$ pigs: The COL diet corresponded to RL diet supplemented with 12 g/kg colestyramine (see detailed composition in **Table S1)**. Polyp number (**a**) and size (**b**) in the distal colon (last 40 cm, 3m = 3 months, one month prior to intervention; 7m = 7 months, end of feeding period). Litters are indicated by different symbols. **c,** Percentage of Ki67+ cells in crypts of the distal colon. N = 4 or 5 pigs per diet. For each pig, 10 randomly selected fields were counted (coloured dots). Mean values and standard deviations per pig are shown in grey. **d,** Exemplary microscopic pictures of Ki67 staining (bars = 200 μm). Statistics: **a** and **b**, Paired Wilcoxon signed rank test; **c** and **d**, Kruskal-Wallis test with Dunn's multiple comparisons and Benjamini-Hochberg adjustment (** p.adj. ≤ 0.01). CTRL, control diet (n = 5); RL, red meat and lard diet (n = 4); COL, colestyramine diet (n = 5).

Fig. 4 Lipid profiles in pig faeces at the end of the feeding period (7 months of age, n = 5 for CTRL and COL, n = 4 for RL). **a**, Mean values of primary (grey) and secondary (brown) BAs. All values are given in **Table S3**. **b**, Individual values for DCA and 12-KLCA. Mean values and standard deviations are show in grey. **c**, Sterol/stanol profiles. **d**, FA profiles: total saturated FA (sat. FA), monounsaturated FA, di-unsaturated FA, >2 unsaturated FA, FAs separated by chain length, branched chain FA (iso- and ante-iso), and total FA. Individual values are provided in **Table S3**. Values in **c** and **d** are shown as individual values (black dots) and mean (bars) + standard deviation (whiskers). Statistics: Kruskal-Wallis test with Dunn's multiple comparisons and Benjamini-Hochberg adjustment (* p.adj. ≤ 0.05).

Fig. 5 Effects of microbial 7αDH activity on BA metabolism, intestinal gene expression, and epithelial cell proliferation in the colon of gnotobiotic mice. BACOMI(7αDH-) lacks the secondary BA producer *C. scindens* (blue bars), which is present in BACOMI(7αDH+) mice (orange bars). **a,** Relative abundances of bacteria in colonic content of mice colonised with the BACOMI consortium with (7αDH+, n = 10, 5 female (F) and 5 male (M) mice) or without (7αDH-, n = 10, 5F/5M) *C. scindens* as measured by targeted qPCR. **b,** Primary (grey) and secondary (brown) BA profile in caecal content quantified using LC-MS/MS (female and male mice are shown separately; the stacked bars indicate mean values; all individual concentrations

are available in **Table S4**). **c, d**, Expression of genes related to (**c**) BA metabolism and (**d**) epithelial cell proliferation and differentiation in the colonic mucosa. **e,** Exemplary images of immunofluorescence staining for Ki67+ cells in colonic crypts of BACOMI(7αDH-) or BACOMI(7αDH+) mice and corresponding quantification shown as barplots (n = 4 mice each). **a, c, d, e** show mean values + standard deviation. In **a**, **c** and **d**, the sex of mice is indicated by different symbols (triangle = male; dots = female). Statistics: Wilcoxon rank sum test with Benjamini-Hochberg adjustment (* p.adj. ≤ 0.05; ** p.adj. ≤ 0.01, *** p.adj. ≤ 0.001, **** p.adj. ≤ 0.0001).

Fig. 6 Effects of bacterial 7αDH on colonic tumorigenesis in gnotobiotic mice treated with AOM/DSS. **a**, Setup of AOM/DSS experiments using BACOMI(7αDH-) mice deprived of 7αDH activity and their BACOMI(7αDH+) counterparts colonised with either *C. scindens* (**b, d, f**, 7αDH-, n = 8-7; 7αDH+, n = 6) or *E. muris* (**c, e, g,** 7αDH-, n =10; 7αDH+, n = 8). Mice were culled after either 16 weeks (*C. scindens*) or 18 weeks (*E. muris*). **b, c,** Relative abundances of the bacterial species in colonic content as analysed by qPCR (**b**) or 16S rRNA gene amplicon analysis (**c**). **d, e,** Primary (grey) and secondary (brown) BA profile in caecal content as quantified using LC-MS/MS (female and male mice shown separately). Data are shown as stacked bar plots of mean values. Individual concentrations are available in **Table S4**. **f**, **g,** Number of colonic tumours; total or stratified according to their size: small (< 1.2 mm^2), medium (1.2 - 2.5 mm^2), large (> 2.5 mm^2). Exemplary macroscopic pictures of the colon are shown below the bar plots; single tumours or areas with many tumours are indicated with red arrowheads or circles. In **b**, **c**, **f**, **g**, the sex of mice is indicated by different symbols (triangle = male; dots = female). Statistical analysis (**d-g**): Wilcoxon rank sum test with Benjamini-Hochberg adjustment (* p.adj. ≤ 0.05; ** p.adj. ≤ 0.01, *** p.adj. ≤ 0.001).

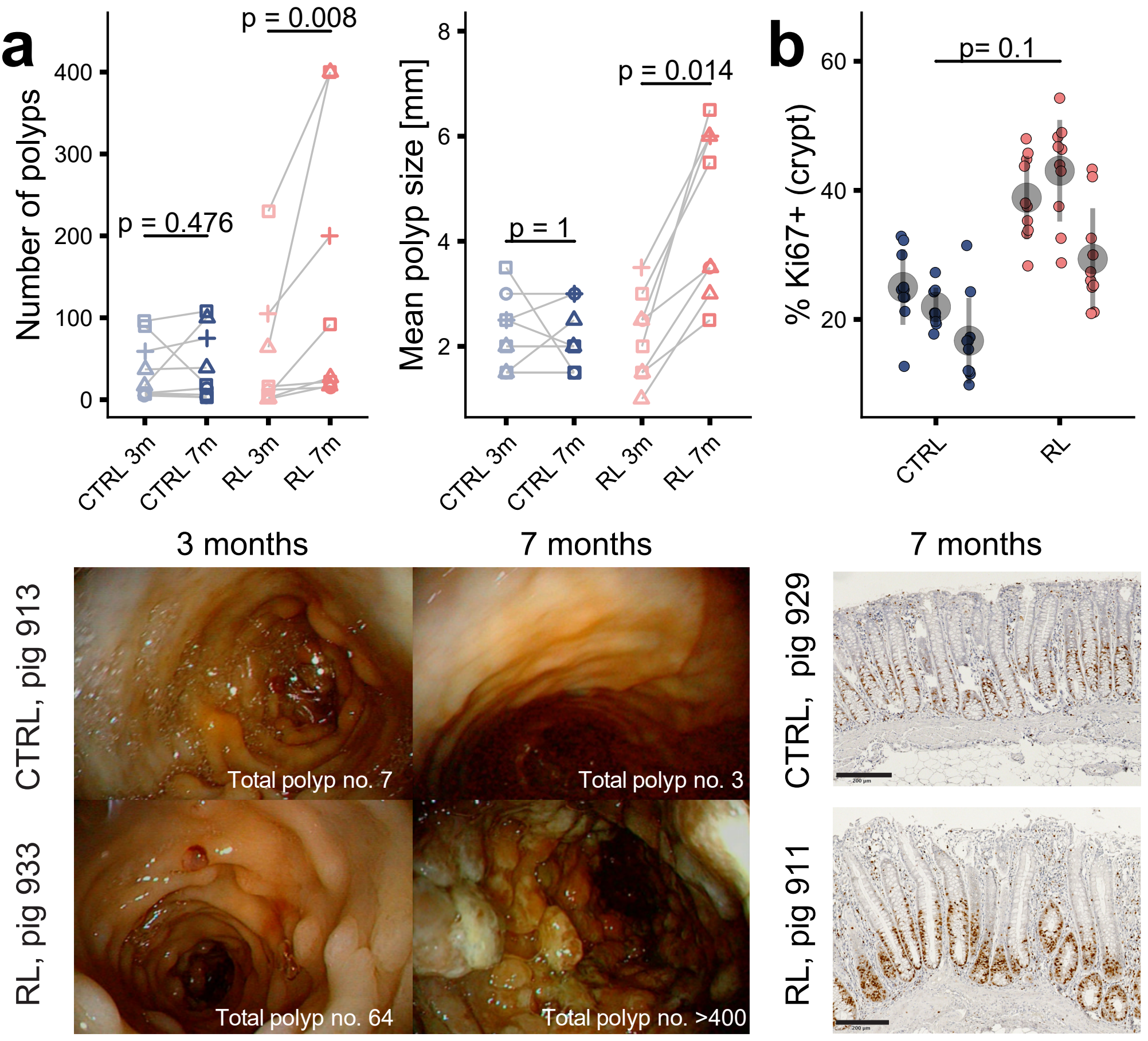
a
Number of polyps
400
300
200
100
0
p = 0.008
p = 0.476
CTRL 3m
CTRL 7m
RL 3m
RL 7m
Mean polyp size [mm]
8
6
4
2
p = 1
p = 0.014
b
% Ki67+ (crypt)
60
40
20
p= 0.1
CTRL
RL
3 months
7 months
7 months
CTRL, pig 913
RL, pig 933
Total polyp no. 7
Total polyp no. 3
Total polyp no. 64
Total polyp no. >400
CTRL, pig 929
RL, pig 911

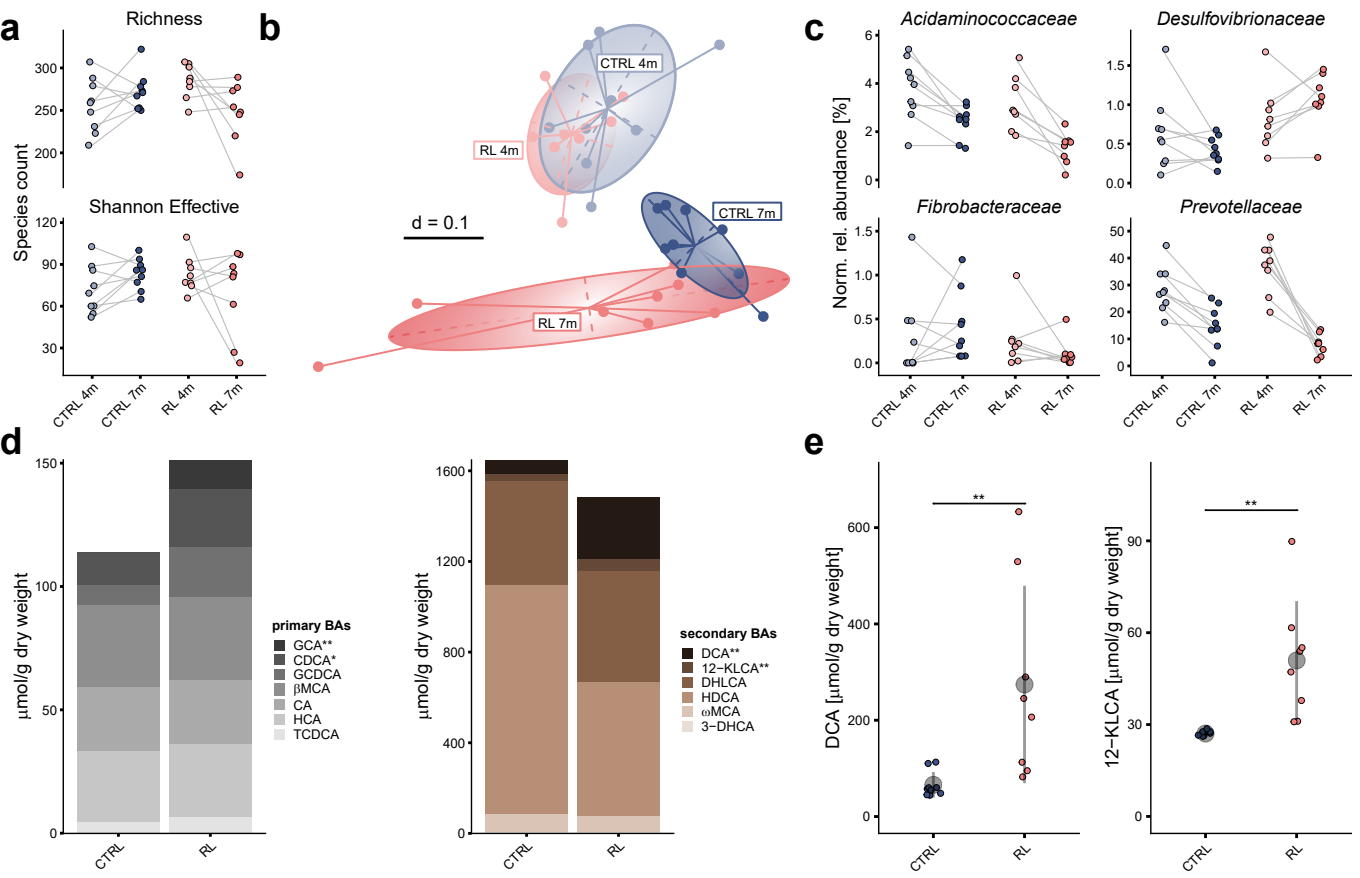
a
Richness
Shannon Effective
Species count
CTRL 4m
CTRL 7m
RL 4m
RL 7m
b
CTRL 4m
RL 4m
CTRL 7m
RL 7m
d = 0.1
c
Acidaminococcaceae
Desulfovibrionaceae
Fibrobacteraceae
Prevotellaceae
Norm. rel. abundance [%]
d
µmol/g dry weight
CTRL
RL
primary BAs
GCA**
CDCA*
GCDCA
βMCA
CA
HCA
TCDCA
secondary BAs
DCA**
12−KLCA**
DHLCA
HDCA
ωMCA
3−DHCA
e
DCA [µmol/g dry weight]
12−KLCA [µmol/g dry weight]
**

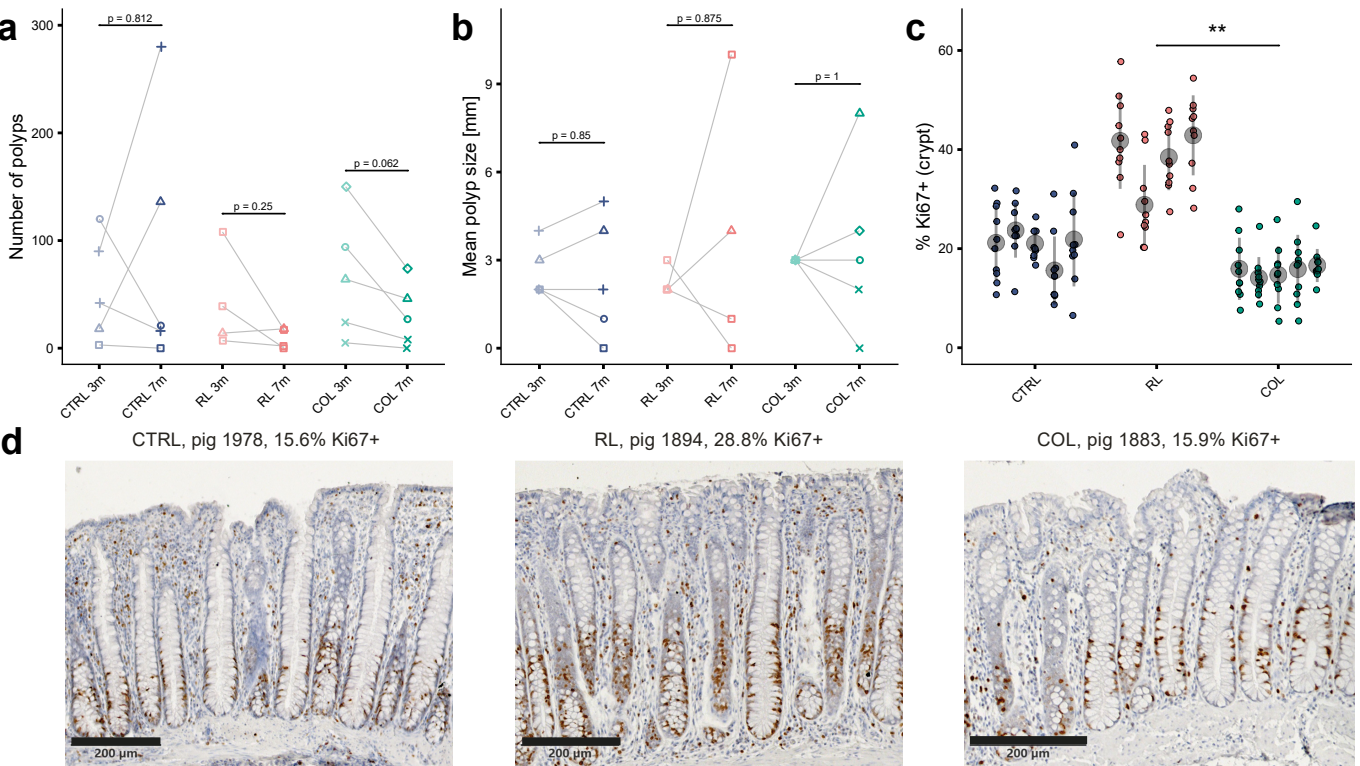
a
Number of polyps
300
200
100
0
p = 0.812
p = 0.25
p = 0.062
CTRL 3m
CTRL 7m
RL 3m
RL 7m
COL 3m
COL 7m
b
Mean polyp size [mm]
9
6
3
0
p = 0.85
p = 0.875
p = 1
CTRL 3m
CTRL 7m
RL 3m
RL 7m
COL 3m
COL 7m
c
% Ki67+ (crypt)
60
40
20
0
**
CTRL
RL
COL
d
CTRL, pig 1978, 15.6% Ki67+
RL, pig 1894, 28.8% Ki67+
COL, pig 1883, 15.9% Ki67+
200 µm
200 µm
200 µm

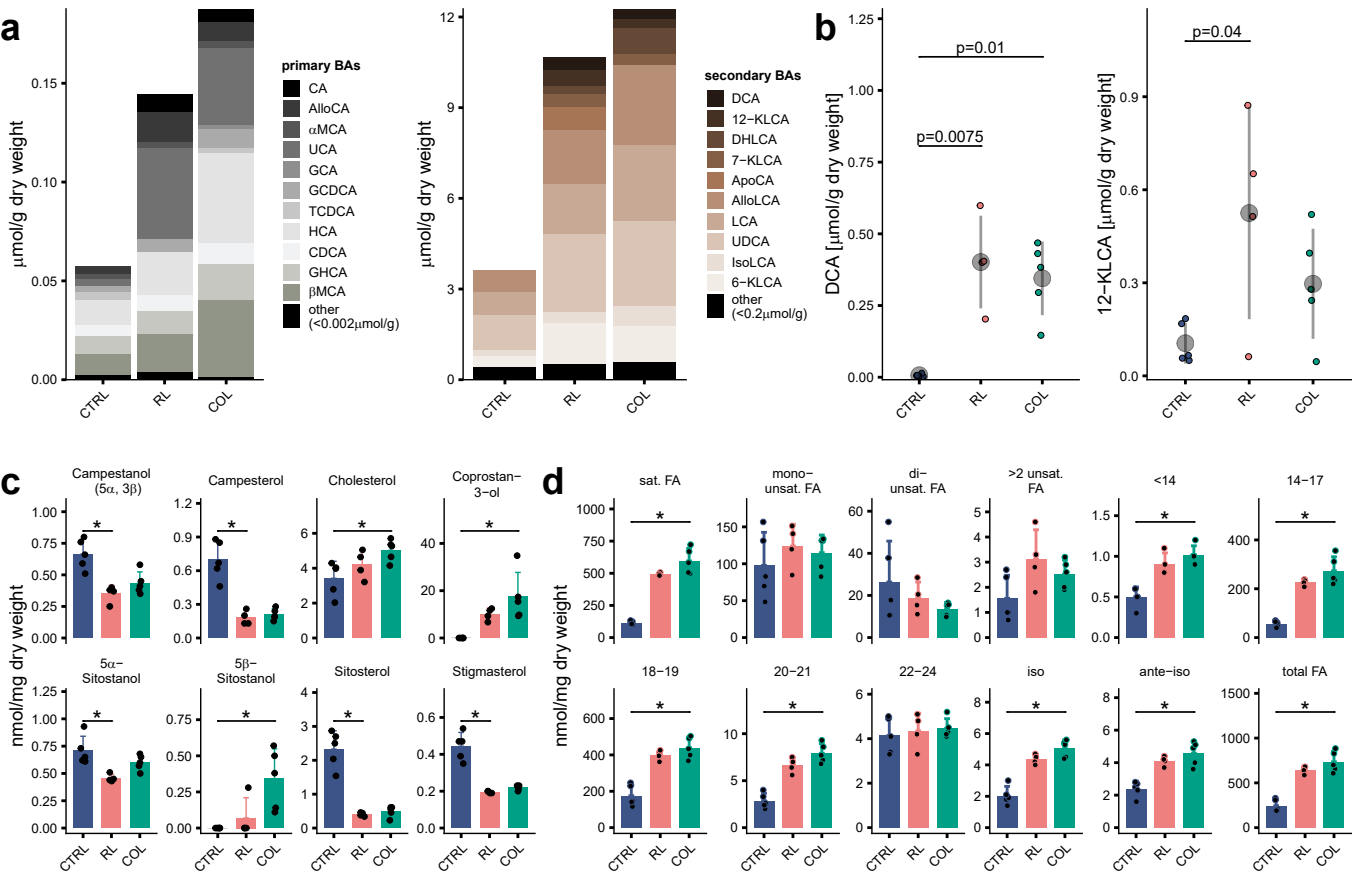
a
µmol/g dry weight
primary BAs
CA
AlloCA
αMCA
UCA
GCA
GCDCA
TCDCA
HCA
CDCA
GHCA
βMCA
other (<0.002µmol/g)
secondary BAs
DCA
12−KLCA
DHLCA
7−KLCA
ApoCA
AlloLCA
LCA
UDCA
IsoLCA
6−KLCA
other (<0.2µmol/g)
CTRL
RL
COL
b
DCA [µmol/g dry weight]
p=0.01
p=0.0075
12−KLCA [µmol/g dry weight]
p=0.04
c
nmol/mg dry weight
Campestanol (5α, 3β)
Campesterol
Cholesterol
Coprostan−3−ol
5α−Sitostanol
5β−Sitostanol
Sitosterol
Stigmasterol
d
sat. FA
mono−unsat. FA
di−unsat. FA
>2 unsat. FA
<14
14−17
18−19
20−21
22−24
iso
ante−iso
total FA

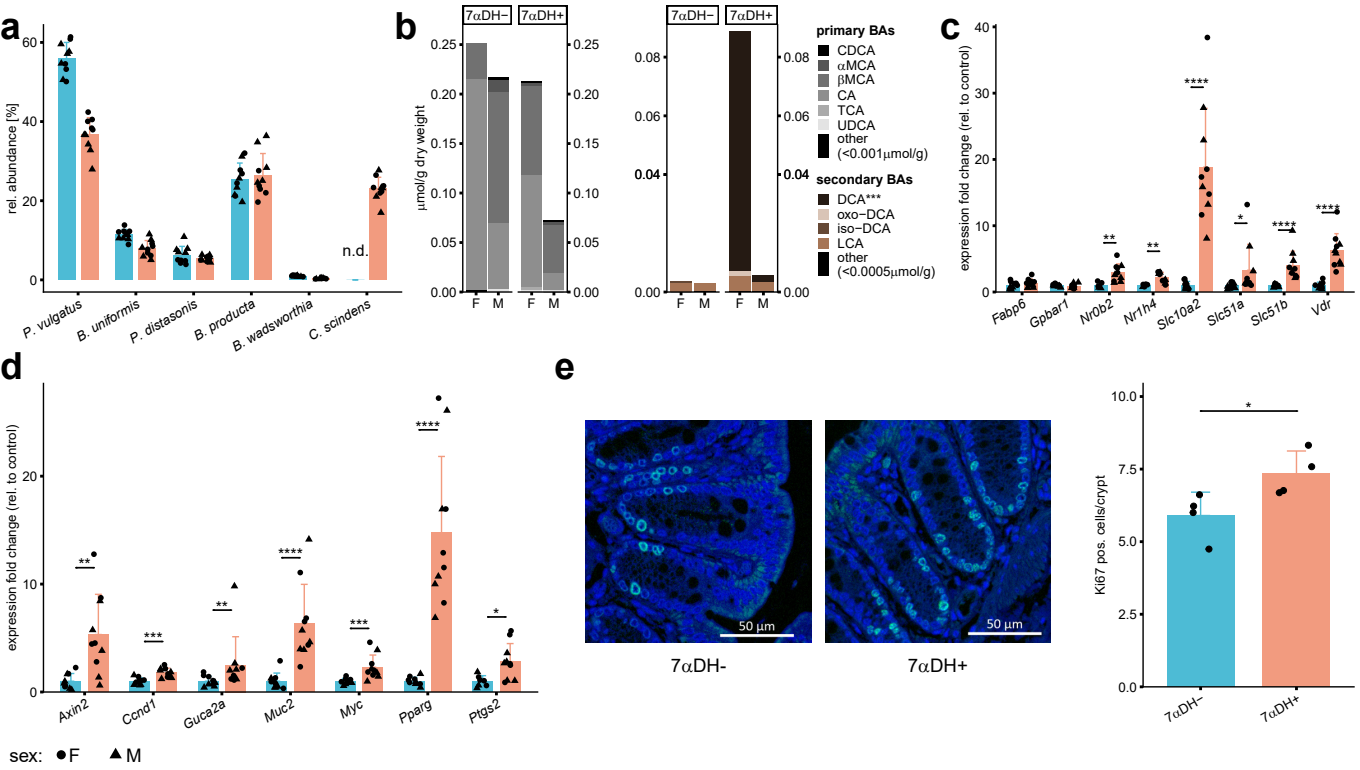
a
rel. abundance [%]
n.d.
P. vulgatus
B. uniformis
P. distasonis
B. producta
B. wadsworthia
C. scindens
b
7αDH−
7αDH+
µmol/g dry weight
F M
primary BAs
CDCA
αMCA
βMCA
CA
TCA
UDCA
other (<0.001µmol/g)
secondary BAs
DCA***
oxo−DCA
iso−DCA
LCA
other (<0.0005µmol/g)
c
expression fold change (rel. to control)
Fabp6
Gpbar1
Nr0b2
Nr1h4
Slc10a2
Slc51a
Slc51b
Vdr
d
expression fold change (rel. to control)
Axin2
Ccnd1
Guca2a
Muc2
Myc
Pparg
Ptgs2
sex: F M
e
50 µm
7αDH-
7αDH+
Ki67 pos. cells/crypt

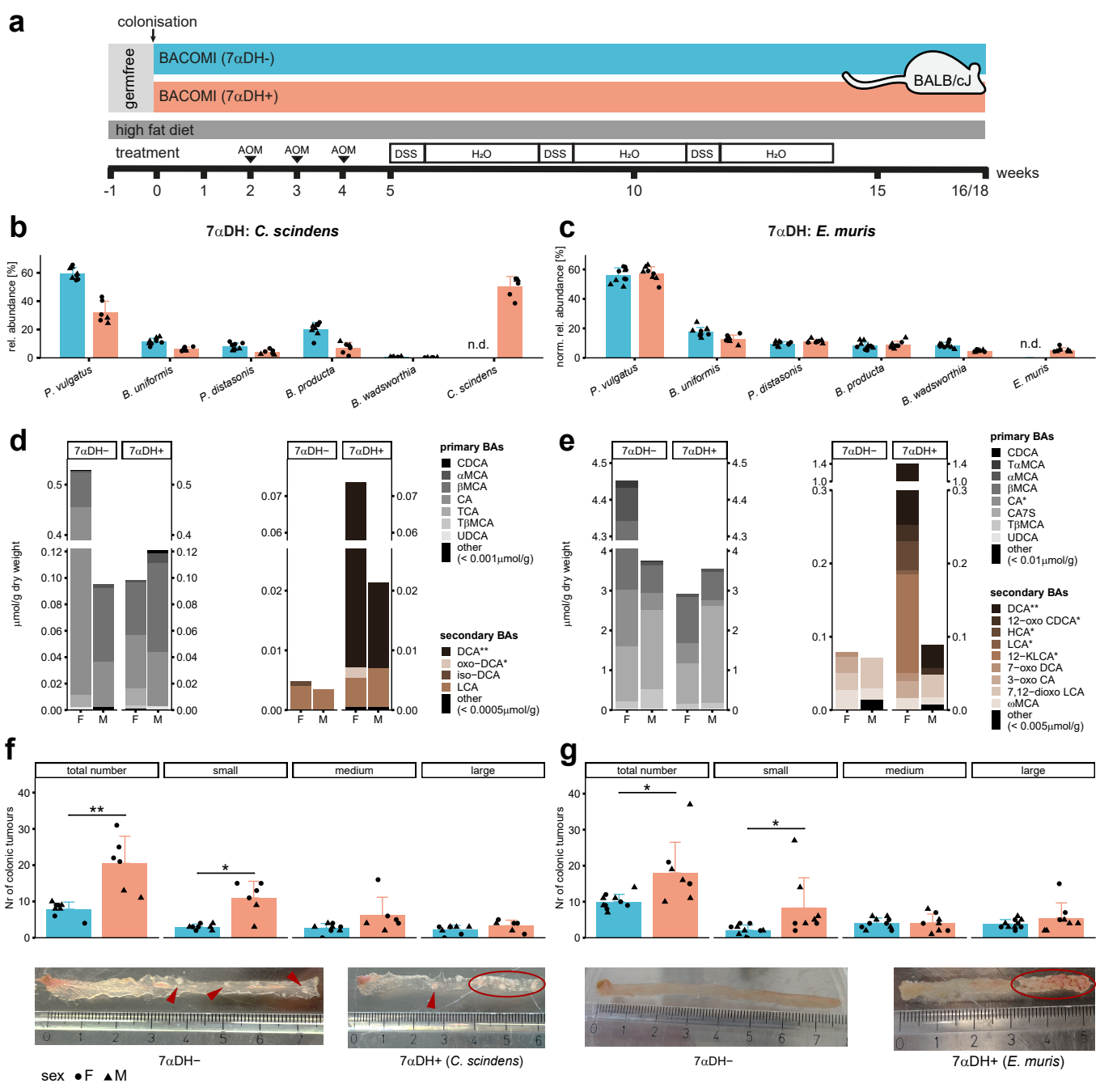
a
colonisation
germfree
BACOMI (7αDH-)
BACOMI (7αDH+)
BALB/cJ
high fat diet
treatment
AOM
AOM
AOM
DSS
H₂O
DSS
H₂O
DSS
H₂O
weeks
-1
0
1
2
3
4
5
10
15
16/18
b
7αDH: C. scindens
rel. abundance [%]
n.d.
P. vulgatus
B. uniformis
P. distasonis
B. producta
B. wadsworthia
C. scindens
c
7αDH: E. muris
norm. rel. abundance [%]
n.d.
P. vulgatus
B. uniformis
P. distasonis
B. producta
B. wadsworthia
E. muris
d
7αDH−
7αDH+
μmol/g dry weight
F
M
primary BAs
CDCA
αMCA
βMCA
CA
TCA
TβMCA
UDCA
other (< 0.001μmol/g)
secondary BAs
DCA**
oxo−DCA*
iso−DCA
LCA
other (< 0.0005μmol/g)
e
7αDH−
7αDH+
μmol/g dry weight
F
M
primary BAs
CDCA
TαMCA
αMCA
βMCA
CA*
CA7S
TβMCA
UDCA
other (< 0.01μmol/g)
secondary BAs
DCA**
12−oxo CDCA*
HCA*
LCA*
12−KLCA*
7−oxo DCA
3−oxo CA
7,12−dioxo LCA
ωMCA
other (< 0.005μmol/g)
f
total number
small
medium
large
Nr of colonic tumours
**
*
g
total number
small
medium
large
Nr of colonic tumours
*
*
7αDH−
7αDH+ (C. scindens)
7αDH−
7αDH+ (E. muris)
sex ●F ▲M